Restructuring effects of the chemical environment in metal nanocatalysis and single-atom catalysis

L. Piccolo

Catalysis Today xxx (xxxx) xxx–xxx

Contents lists available at ScienceDirect

Catalysis Today

journal homepage: www.elsevier.com/locate/cattod

Restructuring effects of the chemical environment in metal nanocatalysis and single-atom catalysis

Laurent Piccolo

Univ Lyon, Université Claude Bernard Lyon 1, CNRS, IRCELYON, F-69626 Villeurbanne, France

ARTICLE INFO

This article is dedicated to the memory of my collaborator and friend, Prof. Roy L. Johnston.

Keywords:
Nanocatalysis
Single-atom catalysis
Restructuring
Dynamic effects
Metal-support interaction
Operando characterization

ABSTRACT

Metal-based heterogeneous catalysts mostly consist of supported nanoparticles of a few nanometers in size, since these objects provide a good compromise between exposed active surface area and structural stability. However, far from being static, heterogeneous catalysts constantly evolve under reaction conditions, thereby creating and removing surface sites in response to their gaseous or liquid reactive environment. Modern *ex situ* and *in situ* investigations have shown that nanocatalysts at work can face a number of deep restructuring phenomena, such as morphological change, compound formation, segregation, leaching, as well as redispersion and other metal-support interaction effects. Recently emerging single-atom catalysts are – like subnanometric clusters – especially sensitive to their chemical environment. Using examples from the recent literature with a particular emphasis on *operando* characterization studies, this article reviews the main dynamic effects induced by the reaction medium on nanocatalysts (including nanoalloy catalysts) and single-atom catalysts.

1. Introduction

Located at the frontier between chemistry and materials science, heterogeneous catalysis has numerous applications in oil refining, chemicals synthesis, pollution abatement, and energy storage/utilization. Realizing that the catalyst composition and structure influence the catalytic performance through the choice of the metal precursor(s) and the preparation method is almost as old as the catalysis concept itself. However, heterogeneous catalysts have long been seen as static playgrounds for catalytic reactions, and the knowledge of restructuring phenomena is much more recent [1]. From post-reaction observation and *in situ* or even *operando* characterization, one has increasingly become aware of the dynamic character of catalytic phases [2–5]. The latter especially holds for so-called "nanocatalysts", i.e. the important catalyst class of nanoparticles (generally metallic and supported) [6–8], since their limited number of atoms provides them with enhanced restructuring possibilities with respect to bulk solids; and their high surface energy can stimulate these changes. At the single atom limit, the influence of the support and the reaction medium on the metal state and its related catalytic performance is even more dramatic [8–11]. The catalyst and its chemical environment should actually be seen as a whole, where the structure of the solid catalyst affects, and is affected by, the nature of the adsorbates and reactant/product molecules (Fig. 1). Understanding these relationships is a prerequisite to select optimal catalysts and catalytic conditions, and even design new catalysts and reactors.

Fig. 2 shows an overview of the restructuring possibilities than can encounter nanoparticles (NPs) in their catalytic – or chemical/reactive – environment (most of these effects will be illustrated in Section 3 with suitable references). The latter encompasses not only the nature of the liquid or gaseous phase, the corresponding concentrations or pressures, the temperature, but also aspects related to the operating conditions such as the reactant/catalyst contact time, and the possible presence of light (photocatalysis) or electric potential (electrocatalysis). Structural parameters such as NP size, lattice structure, shape and composition can deeply evolve during a reaction. The presence of a support (metal oxide, carbon, etc.) leads to additional possible environment effects, such as redispersion and encapsulation.[1] For "large NPs", the phase changes can be limited to the surface top layers. In contrast, "small NPs" ($\sim$2 nm $<$ size $<$ $\sim$5 nm, a few hundreds to a few thousands of atoms), "clusters" (size $<$ $\sim$2 nm, a few to a few hundreds of atoms),[2] or single atoms are inherently highly sensitive to their environment as the metal species may e.g. diffuse and aggregate. Under harsh reaction conditions such as those used in electrocatalysis in acidic media or

E-mail address: Laurent.Piccolo@ircelyon.univ-lyon1.fr.

[1] The support may be also considered as an external perturbator of the NP structure (i.e. part of the NP environment), through e.g. NP truncation with an oxide support. However, in the following, the metal/support couple will be most often treated as a whole.

[2] As there is no global consensus on the definition of "clusters" and "nanoparticles" in terms of size threshold, the mentioned values have been adopted herein to facilitate the discussion. The "size" term here refers to the diameter of the sphere having the same volume as the object.

https://doi.org/10.1016/j.cattod.2020.03.052
Received 12 December 2019; Received in revised form 3 March 2020; Accepted 26 March 2020
0920-5861/

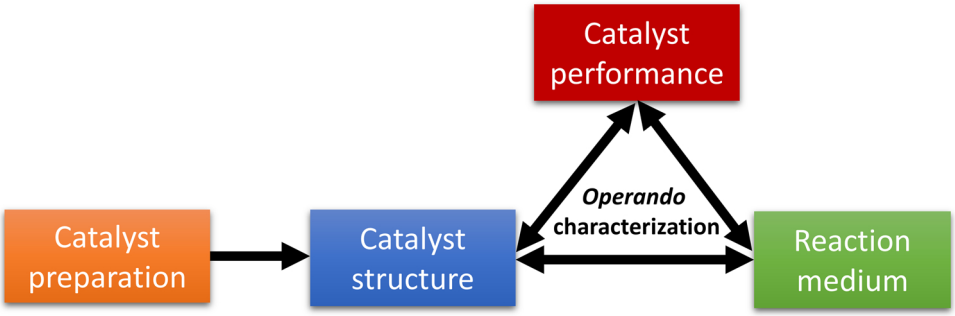

Fig. 1. Scheme of the interplay between catalyst structure, environment ("reaction medium"), and performance.

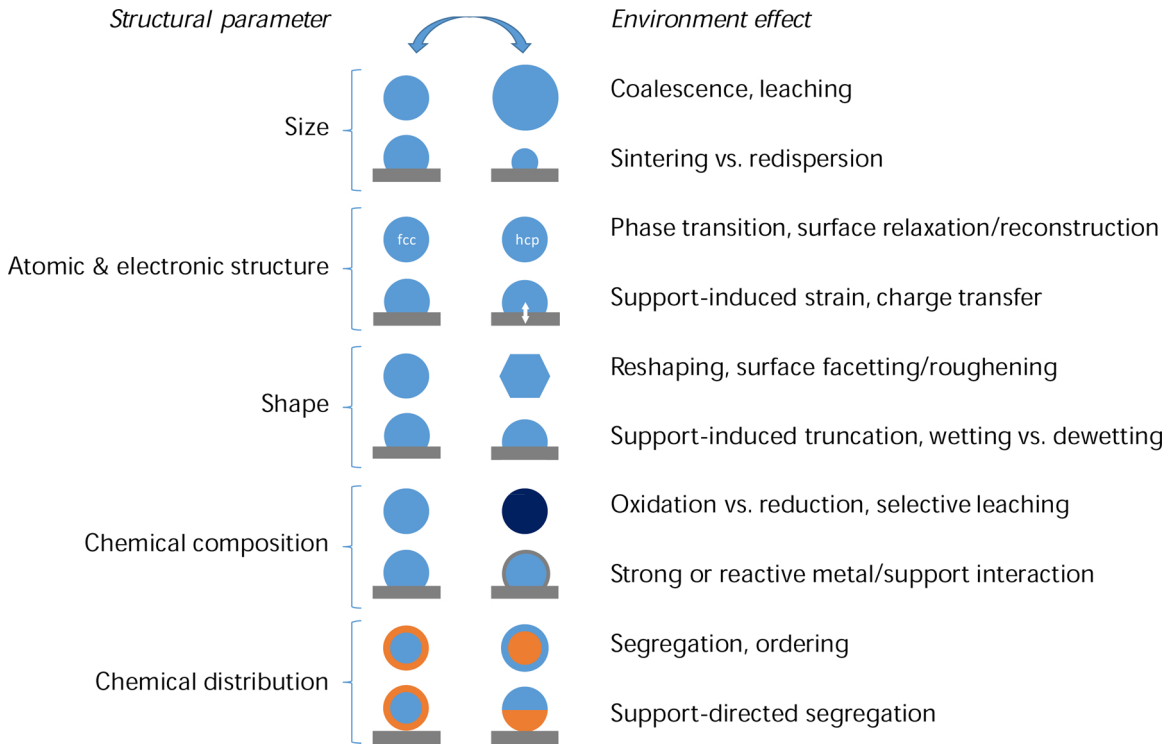

Fig. 2. Examples of NP structural changes induced by the catalytic environment.

under dynamic operation, the metal phase may even lose metal atoms through gradual leaching. The time scales of usually considered catalyst restructuring processes vary between microseconds and years [4], depending on the process and the conditions of operation or storage.

The aim of this paper is to review, in a synthetic way, the various types of restructuring effects of the gaseous or liquid reaction medium on nanocatalysts and single-atom catalysts (SACs). The effects of chemical thermal treatments, such as oxidative calcination and reduction, are also covered. Some results derived from surface-science studies of model planar catalysts are included. Besides many examples from the recent literature, choice has been made to illustrate environment effects with a number of works from IRCELYON, owing both to the vastness of the addressed topic and the context of this special issue. These works include environmental transmission electron microscopy results reported here for the first time. This minireview is mostly focused on "thermal" heterogeneous catalysis, but a few examples concerning electrocatalysis and photocatalysis are also given. After a brief introduction of suitable characterization techniques and computational methods (Section 2), Section 3 reviews environment effects in two subsections, adsorption-induced restructuring and combined adsorption-support effects.

2. *In situ* and *operando* characterization methods

In complement to conventional "*ex situ*" characterization, the spectroscopic or microscopic investigation of catalysts under reactive atmosphere is becoming current practice in laboratories or at synchrotrons. In the specific case where measurements are carried out in catalytic conditions in a dedicated reaction cell with simultaneous measurement of the catalyst performance, such an analysis is called *operando* [12–14] (Fig. 3). In the other cases (single gas or liquid exposure, low-pressure conditions, large chamber volume, simultaneous heating or cooling, etc.), the techniques are referred to as *in situ*,[3] environmental, near-ambient-pressure, or other.

Table 1 lists the most currently employed methods to investigate nanocatalysts – as well as SACs in most cases – in the presence of gases or liquids, and Fig. 4 illustrates the characterization of these two types of catalysts. The next paragraphs provide a quick overview of selected characterization techniques, while the next section will report a number of corresponding examples. For a comprehensive presentation of herein

[3] This term being more generic than "*operando*", it is sometimes used in the present article to refer to catalyst characterization under any reactive environment.

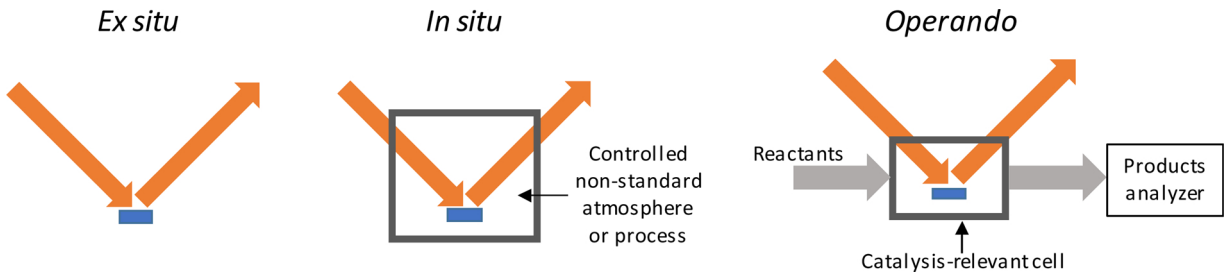

Fig. 3. Illustration of *ex situ*, *in situ* and *operando* catalyst characterization approaches. Orange arrows represent the radiation used for characterization of the sample, depicted in blue.

Table 1
Main *in situ* nanocatalyst characterization techniques, main information they provide, and most suitable ones for *operando* analysis.

Technique [a]	Information	Suitable to *operando* characterization
IR spectroscopy (FTIR, DRIFTS, ATR, IRAS)	Adsorbate nature and amount, adsorption site	✓
Raman spectroscopy (SERS, TERS)	Nanoscale structure	✓
XAS (EXAFS, XANES, QXAS)	Local atomic structure, oxidation state	✓
SAXS (GISAXS)	NP size and morphology	✓
XRD - WAXS (PXRD, SXRD, GIWAXS)	Crystal phase and size, atomic order	✓
XPS (NAPXPS)	Chemical composition, oxidation states	Low pressure, large volume
TEM Environmental TEM	Bulk atomic and chemical structure	Low pressure, large volume
In situ TEM		Low catalyst amount
SPM (STM, AFM…)	Surface structure	Planar model catalysts

[a] Meaning of acronyms. FTIR: Fourier transform infrared. DRIFTS: diffuse reflectance infrared Fourier transform spectroscopy. ATR: Attenuated total reflectance. IRAS: infrared reflection absorption spectroscopy. SERS: surface-enhanced Raman spectroscopy. TERS: tip-enhanced Raman spectroscopy. XAS: X-ray absorption spectroscopy. EXAFS: extended X-ray absorption fine structure. XANES: X-ray absorption near-edge structure. QXAS: quick XAS. SAXS: small-angle X-ray scattering. GISAXS: grazing-incidence SAXS. XRD: X-ray diffraction. PXRD: powder XRD. SXRD: surface XRD. WAXS: wide angle X-ray scattering. GIWAXS: grazing-incidence WAXS. XPS: X-ray photoelectron spectroscopy. NAPXPS: near-ambient-pressure XPS. TEM: transmission electron microscopy. SPM: scanning probe microscopy. STM: scanning tunneling microscopy. AFM: atomic force microscopy.

evoked *in situ* techniques and others (neutron scattering, electron paramagnetic resonance, nuclear magnetic resonance, UV–vis spectroscopy, etc.), the reader may consult suitable books and reviews [15–19].

Characterization techniques most often rely on electron and/or photon probes. Whereas electrons strongly interact with matter and thus have a very limited mean free path in the presence of molecules, photonic vibrational (infrared, Raman) and X-ray techniques are inherently suitable for *operando* investigation. In particular, through the use of a dedicated low-volume reaction cell with heating capability, coupled to an online gas detection device such as a mass spectrometer (MS) or a gas chromatograph (GC), conventional flow-fixed-bed reactor conditions can be mimicked while recording spectroscopic and kinetic data on high-surface-area catalysts.

2.1. Photon-based techniques

Raman spectroscopy, coupled with online GC, has been at the origin of the *operando* spectroscopy methodology proposed by Bañares et al. in 2002 [12]. It is an especially valuable technique for monitoring oxidic, sulfidic or graphitic species at the surface of metal oxides, as well as structural defects such as oxygen vacancies [3,21–27]. Complementary to Raman, IR spectroscopy [28,29], including diffuse reflectance infrared Fourier transform spectroscopy (DRIFTS) [30], is a convenient and powerful method for identifying molecular adsorbates as well as probing the surface metal site nature and oxidation state – when using e.g. CO as a reactant – in reaction conditions [10,31,32]. Optical spectroscopies relying on the localized surface plasmon resonance – including direct [33] or indirect [34] nanoplasmonic sensing, and surface- or tip-enhanced Raman scattering [35] – are also able to reveal dynamic processes at the surface of nanocatalysts.

Synchrotron radiation X-ray absorption spectroscopy (XAS) is widely employed to investigate the local structure of catalysts at work, with time resolution reaching the millisecond range (QXAS). Generally combined, XANES and EXAFS give respectively access to the oxidation state of the chosen metal element and its coordination with neighboring atoms (nature, number, distance), whether belonging to the metal particle itself, the support, or even an adsorbate [10,36,37]. EXAFS is also an invaluable complement to atomic-resolution electron microscopy for gaining statistical (sample-averaged) information on metal dispersion, and thereby checking the homogeneity of SAC samples [20,38]. X-ray scattering techniques [39,40] such as X-ray diffraction [41,42] and small-angle X-ray scattering (SAXS) [43] allow one to determine *in situ* the atomic-level (crystalline phase and domain size, atomic order/disorder) and nanoscale (NP size, shape and spatial distribution) structural characteristics of nanocatalysts, respectively, in the course of their elaboration or evolution under catalytic conditions. Wide angle X-ray scattering (WAXS) appears better suited to investigate inhomogeneous atom arrangements in weakly crystalline nano-objects (e.g. disordered nanoalloys), especially by using the atomic-pair-distribution function (PDF) analysis procedure [42,44]. Notably, SAXS and WAXS can be employed simultaneously, using the same setup [45,46]. Finally, anomalous X-ray scattering techniques combine the advantages of absorption and scattering methods to provide information on atom rearrangements at several scales with element specificity [40,44,47].

Near-ambient pressure X-ray photoelectron spectroscopy (NAPXPS), a hybrid photon-in/electron-out surface-sensitive technique, is a recent evolution of XPS for probing the near-surface region of planar or powder catalysts under reactive gaseous environments, generally at low pressure ($<$ ~20 mbar) [48–50]. Recent developments of NAPXPS even allow analyzing solid-vapor and solid-liquid interfaces, and thereby investigating electrochemical processes [51–54]. NAPXPS can use a laboratory or a synchrotron X-ray source, and provides information not only on the catalyst surface composition and oxidation states, but also on the nature of the adsorbates and the gas-phase species close to the surface [55].

Besides XPS, surface-science techniques such as scanning probe microscopies like STM [56], and adaptations of X-ray and IR techniques

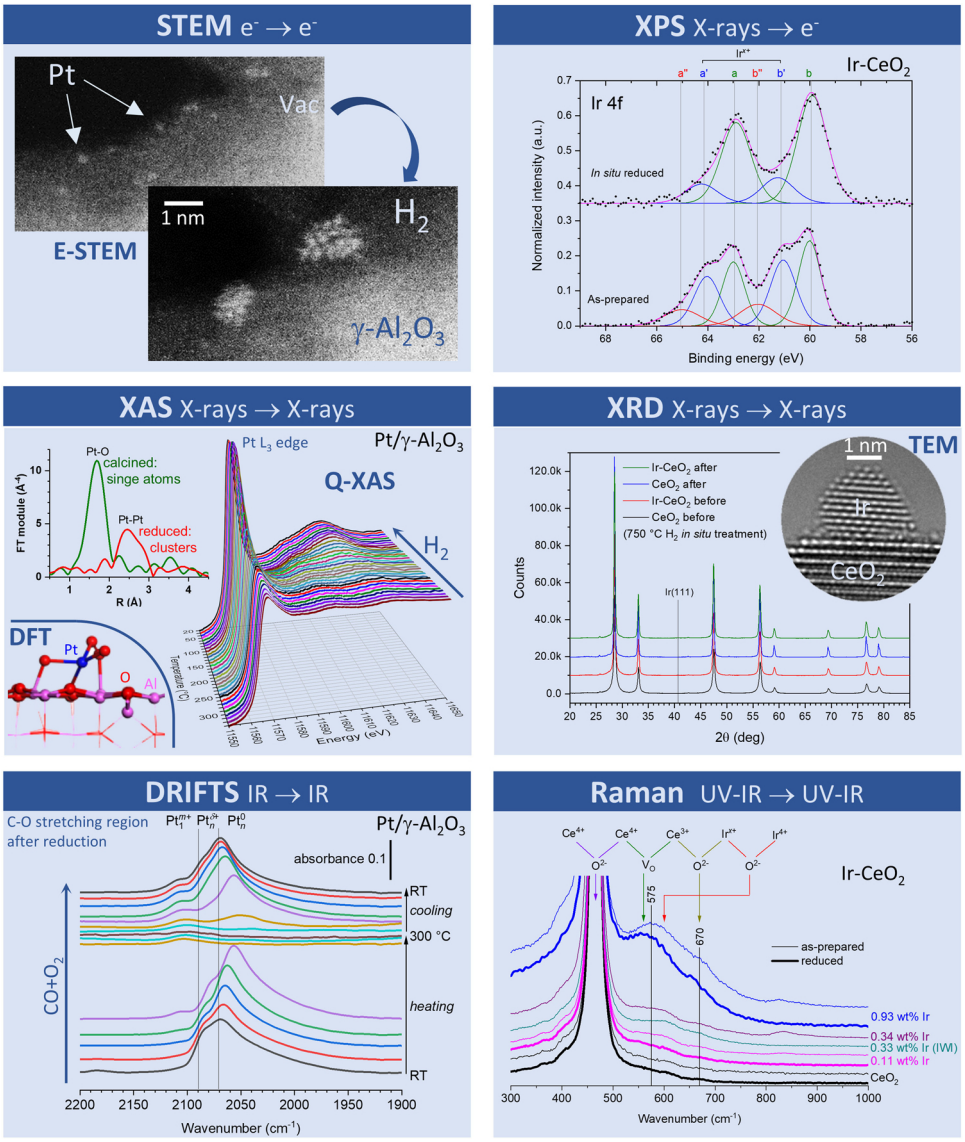

Fig. 4. Examples of in situ characterization of supported nanocatalysts and single-atom catalysts. The left-hand-side panel corresponds to Pt/Al_2O_3 SACs (adapted from Refs. [10,20]), while the right-hand-side panel relates to Ir/CeO_2 catalysts synthesized by one-step solution combustion (adapted from Ref. [21]). Incoming and outcoming radiation types are indicated. Acronyms are explained in Table 1.

to planar systems such as GISAXS [39,43], SXRD [57,58] and IRAS [59], provide valuable information on the interaction of model catalysts with chemical environments [6,60].

2.2. Transmission electron microscopy

The recent emergence of aberration-corrected transmission electron microscopes (TEM) [61,62] has allowed gaining unprecedented atomic-scale insight into nanocatalyst structure and dynamics, and contributed significantly to the advent of single-atom catalysis. Two types of devices permit the direct observation of catalysts in reactive environments [63]. In a dedicated environmental TEM (ETEM), gases at low pressure ($<\sim$20 mbar) are introduced directly into the microscope column thanks to a system of apertures and differential pumping, which restrains the introduced gas to the specimen surroundings, and preserves high vacuum in the other parts of the column as well as ultrahigh vacuum (UHV) at the electron source. Two advantages of this type of instrument are the ultimate spatial resolution attainable, similar to the one in high-vacuum analysis [64], and the possible use of any type of specimen holder, allowing e.g. heating, cooling, biasing, or tomographic imaging [65,66].

Alternatively, dedicated sample holders equipped with an electron-transparent cell allow one to work at higher pressure (up to several bars) [67] or in liquid phase [68–70][4] within conventional high-vacuum TEM columns. While dedicated holders provide several orders of magnitude higher pressures than an ETEM and permit online MS monitoring, the sample area of investigation is limited compared to conventional TEM grids, and the electron-transparent windows constraining the gas lower the spatial resolution.

To access chemical contrast, TEM is increasingly performed in scanning mode (STEM) with high-angle annular dark field (HAADF) detection ("Z-contrast"), and often supplemented by energy-dispersive X-ray spectroscopy (EDXS), electron energy-loss spectroscopy (EELS), or energy-filtered TEM (EFTEM) imaging [72,73].

[4] This includes electrocatalytic conditions though there exists limitations due to the strong interaction of the electron beam with the electrochemical medium [71].

2.3. Computational modeling

Theoretical modeling of catalytic processes has long relied on low-coverage adsorption of molecules on periodic single-crystal surfaces or few-atom clusters at zero Kelvin and in vacuum. This approach, mostly based on the density functional theory (DFT), has been successful in uncovering reaction mechanisms and active sites at the atomic scale, and sometimes discovering efficient catalysts [74]. Nowadays, in synergy with the experimental approach, multiscale computational modeling (including computational thermodynamics, molecular dynamics, and microkinetics), recently helped by machine learning, can account for the interaction of complex solid catalysts with realistic reaction environments [75–77]. Beyond temperature and pressure, the complexity of dynamic catalytic systems is increasingly considered through e.g. support, reactant concentration, coverage and solvent effects, towards *operando* computational modeling [4,75–80].

3. Overview of environment effects

3.1. Adsorption-induced restructuring

3.1.1. Surface atomic restructuring: single crystals and large nanoparticles

Gold is the noblest of all the metals [81]. However, IRAS and STM experiments have shown that even the most stable, close-packed (111) surface of Au single-crystals chemisorbs CO, the classical probe molecule, though at relatively high partial pressure ($> \sim 1$ mbar at RT) [59]. CO adsorption induces a surface restructuring consisting in step-edge roughening and lifting of the $22 \times \sqrt{3}$ "herringbone" reconstruction. In the case of the more open Au(110) surface, the roughening is even more dramatic [82]. DFT calculations have shown that the elevated CO pressure enables the surface diffusion of Au-CO entities [83]. The formation of low-coordination Au sites is in turn favorable to CO chemisorption, as surface steps and kinks bind CO twice stronger than terraces [59]. In relation to this phenomenon, CO chemisorption has been suggested to reconstruct Au NPs [29], and to "pull out" Au atoms from particles [84,85]. Gold atoms may even detach from nanocatalysts supported on reducible oxides (CeO_2, TiO_2) in CO oxidation conditions through a reversible dynamic process [86,87].

Unsurprisingly, adsorption-induced surface roughening/clustering has been observed for other metals, e.g. in the cases of CO chemisorption and oxidation on Pt single-crystals investigated by *in situ* STM [88,89]. On supported nanoparticles, adsorption may cause additional phenomena owing to the simultaneous presence of facets of several orientations, as well as edges and corners. The effect of CO adsorption on the surface structure of carbon-supported Pt nanoparticles has been investigated by Avanesian et al. through a combination of *in situ* TEM, DRIFTS and DFT-based modeling [67]. The authors have revealed a reversible, facet-selective reconstruction under elevated CO pressure: the minority (100) facets of the initial truncated octahedra roughen into vicinal stepped facets upon CO adsorption, whereas the (111) facets remain intact, which leads to an overall rounding of the nanoparticles (Fig. 5).

Similar shape variations have been identified by *in situ* TEM for several supported metals (Au, Cu, Pd, etc.) under oxygen, hydrogen or reaction conditions, when changing the reactive atmosphere or the partial pressure(s) [90–95]. In all these cases, adsorption effects on the nanoparticle morphology can be well understood by considering arguments only based on surface/interface thermodynamics, such as minimization of the facet-dependent surface tension. This also holds for nanoparticles strongly anchored on a support, where the equilibrium morphology, including the particle truncation induced by the substrate, can be accounted for by the Wulff theorem and the interface energy [96] (see also Section 3.2.1).

In turn, the NP shape/morphology obviously drives the catalytic performance, in such a way that NP shape control allows a tuning of the catalytic performance, as e.g. in the cases of CO + NO reaction [97] and butadiene hydrogenation [98,99] on palladium. Imbihl and Ertl demonstrated oscillatory (bistable) CO oxidation kinetics on extended Pt single-crystal surfaces under steady-state conditions at low pressure ($\sim 10^{-4}$ mbar), which was correlated to periodic adsorption-induced surface reconstruction [100]. More recently, in line with these early works, an oscillatory morphology of large Pt NPs has been visualized by *in situ* TEM during CO oxidation at 1 bar and ca. 700 K in a microreactor coupled to a mass spectrometer [101]. The reaction rate is synchronous with a periodic refacetting of the Pt NPs, which is explained, through a model using DFT and mass transport calculations, by site-dependency of the CO adsorption energy and oxidation rate.

3.1.2. Bulk atomic restructuring: small nanoparticles and clusters

In certain conditions, the small size of the particles ($< \sim 5$ nm) may facilitate their global restructuring owing to the enhanced surface contact with the reactants and the decreased mass transport needed as compared to large NPs. An illustration is provided by the *in situ* time-resolved XAS study of Eslava et al. showing the reversible 2D-to-3D shape transition of Ru-Cs NPs (ca. 2 nm) in graphite-supported Fischer-Tropsch catalysts upon changing the atmosphere from H_2 to CO, pointing to strong CO adsorption [102].

Au/TiO_2 is a popular low-temperature CO oxidation catalyst [103]. In the example of Fig. 6, Au NPs (size $3-4$ nm) supported on rutile TiO_2 nanorods [104] were investigated by ETEM at 300 °C in the presence of oxygen at low pressure (0.5 mbar). It was observed that the fcc particle morphology switches from truncated octahedron (TO) to decahedron (Dh), then back to TO (see also supplementary movie S1). The respective effects of the temperature, the oxygen pressure, the support and possibly the electron beam are difficult to evaluate. However, such a morphological instability has been predicted by DFT calculations for fcc metal particles [105–107]. The stability of a given morphology is size- and metal- dependent, but above a few nanometers the TO and Dh shapes of Au (and Pd) particles have similar stabilities, consistently with our ETEM observations. The icosahedral structure is favored only at smaller sizes, especially for Ni [108] and Cu [109].

The prototypical $Pt/\gamma\text{-}Al_2O_3$ system, which is relevant to industrial hydrocarbon reforming, has been the subject of many experimental and theoretical investigations. Supported subnanometric Pt clusters are extremely sensitive to the reactive atmosphere, which can induce changes in Pt-Pt bond length, electronic structure, shape, size, etc. [110–118]. For example, DFT modeling has shown that bare Pt_{13} clusters exhibit a bilayer structure with Pt-Al and Pt-O bonding to the support [119]. In contrast, in the presence of H_2 at high pressures and/or at low temperatures, the clusters adopt a cuboctahedron shape surrounded by a hydrogen shell, leading to weak cluster interaction with alumina [111,115]. This has been recently confirmed by ETEM experiments, showing an enhanced Pt cluster mobility at low temperature, i.e. when the hydrogen coverage is high [20].

3.1.3. Segregation in nanoalloys

Bimetallic catalysts often exhibit superior catalytic performances with respect to pure metals [6,120–122]. In the case of multimetallic nanoparticles, i.e. nanoalloys, one has to consider an additional structural parameter with respect to monometallic particles, namely the chemical structure, i.e. the atomic structure including the chemical arrangement (or "distribution") of the elements. Nanoalloys may present various configurations, ranging from ordered alloy types (including intermetallic compounds) to core-shell and Janus types [123,124].

The most evident effect of molecular adsorption on an alloy surface is the possible change of its composition through "adsorption-induced surface segregation" [6]. In general, upon adsorption, and provided the temperature is high enough, the element that forms the strongest bonds with the considered adsorbate diffuses toward the surface, which stabilizes the whole system [80]. This phenomenon has been widely studied on extended single-crystal surfaces. For example, in the case of $Pd_{70}Au_{30}$ surfaces, we have shown by low energy ion spectroscopy

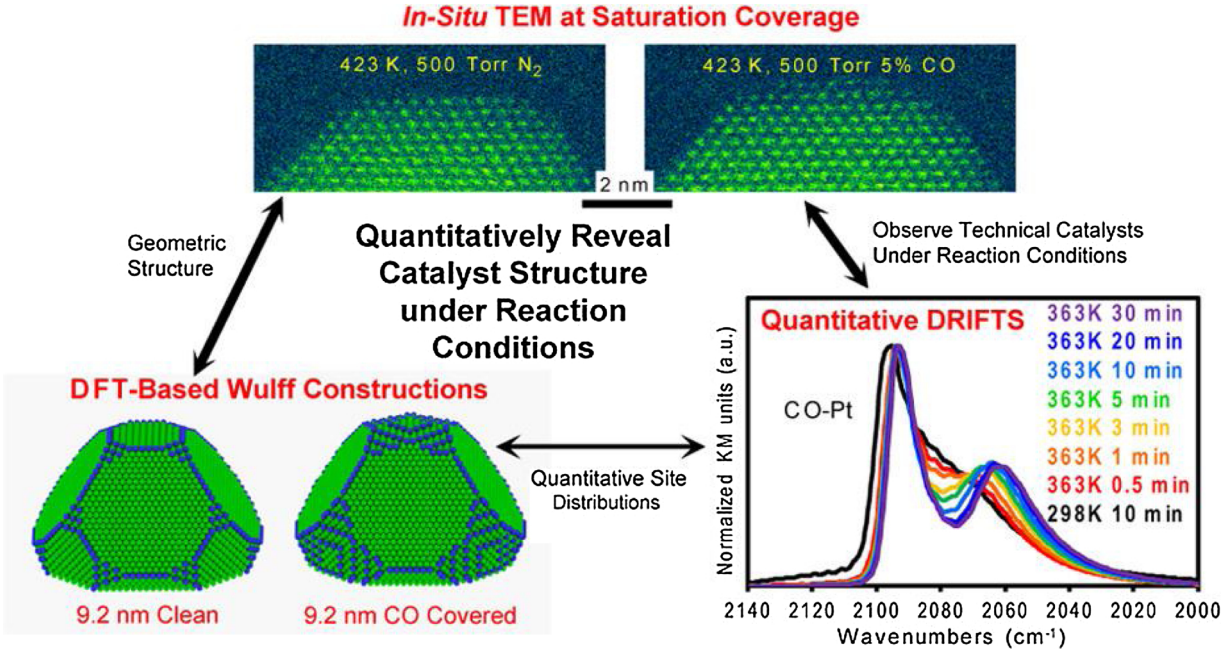

Fig. 5. Illustration of the facet-selective surface reconstruction of carbon-supported Pt nanoparticles under CO pressure. Reprinted with permission from Ref. [67]. Copyright 2017 American Chemical Society.

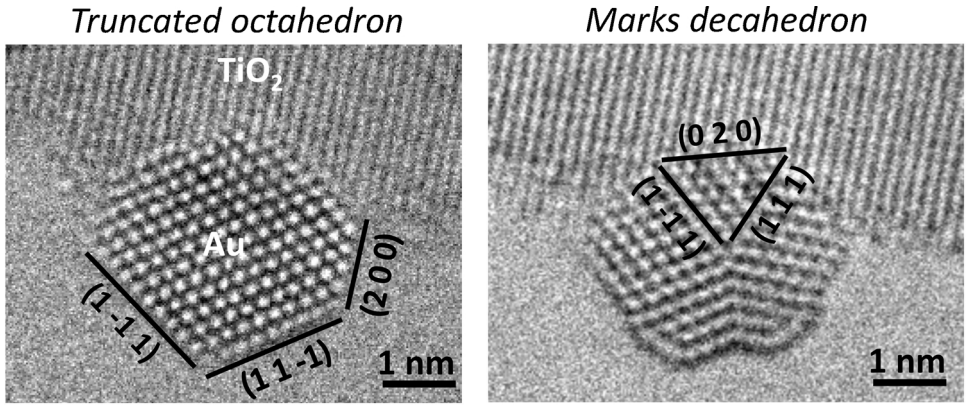

Fig. 6. Aberration-corrected ETEM images (FEI Titan ETEM G2 300 kV) showing the (reversible) shape change, from truncated octahedron to Marks decahedron, of a gold nanoparticle supported on rutile TiO_2 at 300 °C under 0.5 mbar O_2.

(LEIS) that the topmost layer contains ca. 80 % Au after annealing under UHV. However, under a reactant mixture of hydrogen and butadiene – introduced in the mbar range in a dedicated reactor [125] – the surface composition gradually approaches the bulk one ("segregation reversal"), and the catalytic activity increases [126].

By exposing colloidal PdRh nanoparticles to alternating NO and CO + NO atmospheres, Tao et al. have evidenced oscillations of the surface composition by NAPXPS [127]. The segregation process can be facet-dependent, as observed by Dai et al. using *in situ* TEM for Pt_3Co nanoparticles exposed to oxygen at high temperature [128]: cobalt segregates to the surface and gets oxidized at {111} facets, but not at {100} ones. Moreover, as shown by Zhu et al. through DRIFTS experiments and DFT calculations on Au-rich Au-Pd clusters in the presence of CO, adsorption-induced surface segregation can also be favored at the particle edges [129].

3.1.4. Compound formation including oxide, sulfide and carbide

Beyond chemisorption, the interaction of metal nanoparticles with a reactive atmosphere under catalytic conditions may lead to the formation of a near-surface or even a bulk compound, such as oxide, sulfide, etc. If this transformation is gradual under stationary conditions, a continuous activation or deactivation may be observed, depending on the relative activities of the metal and compound phases. For example, we have shown that the sulfidation of Rh during tetralin hydrogenation in the presence of H_2S traces increases Rh activity, whereas Au nanoalloying with Rh prevents its sulfidation and thereby limits its activity; the behavior of Pd is opposite, as the formed PdS_4 phase is less active for aromatics hydrogenation than the reduced metal [130]. Under dynamic (fluctuating) conditions such as those used by Mutz et al. for CO_2 methanation, fast bulk oxidation of supported Ni particles was revealed by *operando* XAS upon removal of H_2 from the gas stream, leading to lower catalyst performance in the subsequent reaction cycle [131].

A lively debate concerns the nature of the (most) active phase – metal or oxide – in CO oxidation over platinum-group metals (Pt, Pd, Rh) [132–134]. An *operando* DRIFTS-MS comparison between Pt/CeO_2 and Rh/CeO_2 catalysts suggests that the CO oxidation activity of Pt is highly sensitive to its oxidation state, which itself depends – unlike for Rh – on the reaction conditions; more reducing conditions are more favorable [32]. Oxidation and reduction are the most obvious

environment effects in nanocatalysis, and reports on structural effects of these processes are countless.[5] Nevertheless, the recent development of aberration-corrected ETEM now permits their direct visualization at atomic resolution, as in the example of copper [137]. In the case of nanoalloys, oxidation and reduction can be coupled with phase segregation [33,55,128,138,139].

Besides the usual negative role of carbon as a surface poison, subsurface diffusion of atomic carbon –from fragmented feed molecules – during alkyne hydrogenation over palladium has been reported to promote the catalytic selectivity by Teschner and coworkers using *in situ* XPS experiments [140–142]. Actually, according to the theoretical work of Piqué et al., the accommodation of carbon atoms in the subsurface region would be favorable for most late transition metals [143]. The influence of carbide phase formation at the surface of cobalt on Fisher-Tropsch catalysis is a long-standing debate [56,144].

3.1.5. Hydrogen absorption and hydriding

A less documented case is the subsurface diffusion/absorption of chemisorbed hydrogen atoms in metal NPs and its influence on surface catalysis. Palladium is the only noble metal absorbing hydrogen to significant extent by forming a β phase hydride (i.e., showing a plateau in pressure-composition isotherms) under mild conditions [145]. However, at small particle sizes, hydrogen has been reported by Kobayashi et al. to diffuse in metals such as Rh and Ir [146,147]. Furthermore, Zlotea et al. have shown that carbon-supported 1 − 2 nm-sized Rh NPs even form a stable hydride at low H_2 pressure and RT [148,149]. The Rh hydride catalysts appeared more active than their metallic counterparts for the partial hydrogenation of butadiene, while retaining a similar selectivity to butenes [150]. The enhancement was ascribed to the stabilization of Rh–H bonds at the NP surface in the presence of subsurface hydrogen, after the theoretical work of Neyman and coworkers [151]. The drastic influence of subsurface hydrogen – and in some cases its interplay with subsurface carbon – on hydrogenation reactions was previously evidenced from surface-science studies of Ni and Pd-based systems [126,152–159].

Beyond downsizing, nanoalloying is an additional way of boosting the hydrogen absorption capacity, as shown for Pd-Pt and Ag-Rh systems [160]. In contrast, we have found that nanoalloying Pd with Ir strongly decreases the hydrogen absorption capacity of Pd and suppresses β hydriding [161,162] through the formation of a core-shell Ir@Pd structure (Fig. 7, left-hand side) [163,164]. The decreased hydrogen capacity is correlated to a strongly increased preferential CO oxidation activity in the presence of H_2 (PROX process) with respect to pure Pd and Ir counterparts (Fig. 7, right-hand side) [161,165]. This Pd-Ir synergy was ascribed to the detrimental effect of hydrogen absorption on the PROX performance of supported Pd nanocatalysts [166,167], as near-surface hydrogen is prone to react with oxygen to form water, making Pd an unselective catalyst [168].

3.1.6. Leaching and restructuring under liquid-phase conditions

A large fraction of *operando* investigations reported in the last years concerns electrocatalysis [19,169], as it often employs severe reaction conditions, e.g. very acidic or alkaline electrolyte and alternation of oxidizing/reducing conditions through potential cycling, generally leading to catalyst degradation. As shown by identical location TEM (IL-TEM) on supported electrocatalysts, this can occur via a number of processes, such as particle oxidation or reduction, detachment, dissolution, and agglomeration [71,170,171]. Recently, Ortiz Peña et al. monitored *in situ* by electrochemical TEM the oxygen evolution reaction (OER) on Co_3O_4 NPs in alkaline or neutral electrolyte. Their results show the irreversible amorphization of the NP surface, leading to a more active phase [70]. Asset et al., using STEM-EDX and *operando* wide-angle and small-angle X-ray scattering, found that carbon-supported hollow Ni-Pt NPs gradually collapse and lose Ni during ageing in oxygen reduction reaction (ORR) conditions [172]. Pavlišič et al., investigating the selective leaching of Cu from $PtCu_3$ NPs in ORR conditions, reported that dealloying is less detrimental to electrocatalytic activity when the bimetallic NPs are atomically ordered, since in that case Pt atoms would retain significant Pt-Cu coordination [173]. A number of studies combining the measurement of electrocatalytic performance in a flow cell and on-line analysis (e.g. inductively coupled plasma MS to quantify dissolution products in the electrolyte [174]) or *in situ* characterization (e.g. FTIR to monitor molecular adsorbates or products [175,176]) have also been reported.

Dissolution phenomena are obviously not limited to electrocatalysis. For example, Khanh Ly et al. recently observed a partial leaching of Re from $ReO_x/Pd/TiO_2$ nanocatalysts after exposure to air and introduction into an aqueous solution of succinic acid [177]. Notably, subsequent pressurization of the batch reactor with 150 bar H_2 (to perform acid hydrogenation) led to Re redeposition, providing an *in situ* method for the preparation of bimetallic catalysts from their Pd/TiO_2 parents.

3.2. Combined adsorption and support effects

The role of a catalyst support – typically a solid oxide – is to stabilize isolated metal particles and thereby maximize the total amount of surface metal sites available for catalysis. Beyond this primary role, the support influences the metal active phase geometrically (wetting, strain, etc.) and/or electronically (charge transfer), and can even directly participate in the catalytic reaction (spillover, bifunctionality, etc.) [20,113,178–183]. The support can be itself modified by the surrounding reaction medium through e.g. the formation of oxygen vacancies or surface functional groups [24,184]. In the case of metal/oxide systems, adhesion energy increases with metal oxophilicity, which suggests that metal-oxygen bonds dominate interfacial bonding [185,186]. Moreover, reducible oxides such as CeO_2 bind metals more strongly than irreducible oxides such as MgO [187]. Overall, the control of metal-support interactions, primarily through the choice of the support nature (composition, morphology) and its modification (doping, surface functionalization, coating), is a way to enhance catalytic performances [183,188]. This enhancement was found prominent for NPs smaller than 4 nm [183].

3.2.1. Wetting and dewetting

With respect to a free nanoparticle in thermodynamic equilibrium, the presence of a support induces NP truncation, the extent of which depends in first approximation on the NP and support surface and interface energies according to the Wulff-Kaishev law [189]. Consistently with this rule, Duan et al. have recently shown using multiscale modeling coupled with *in situ* TEM that the adsorption of H_2 on $Pt/SrTiO_3(110)$ leads to a decrease in the metal/support interface area [96]. Such an adsorption-induced change of NP wetting on the support had been previously observed in the case of Cu/ZnO [90,190]. In turn, this phenomenon affects the nature of perimeter sites, which can play an important role in catalysis. In addition, if the particle is in epitaxy on its support,[6] the interfacial stress can modify the overall equilibrium shape of the particle, together with the bulk and interface structures [189,192].

3.2.2. Support-directed segregation in nanoalloys

Another interesting structural effect of the nanoparticle

[5] A striking possible effect of metal compound (including alloy) formation is to generate hollow NPs via the Kirkendall effect: outward diffusion of metal atoms from the core is faster than inward diffusion of reactive species, resulting in void formation [135,136]. This effect can also be used for metal redispersion [25].

[6] This refers to the case of crystalline support and NP, with a well-defined orientation between their lattices [191].

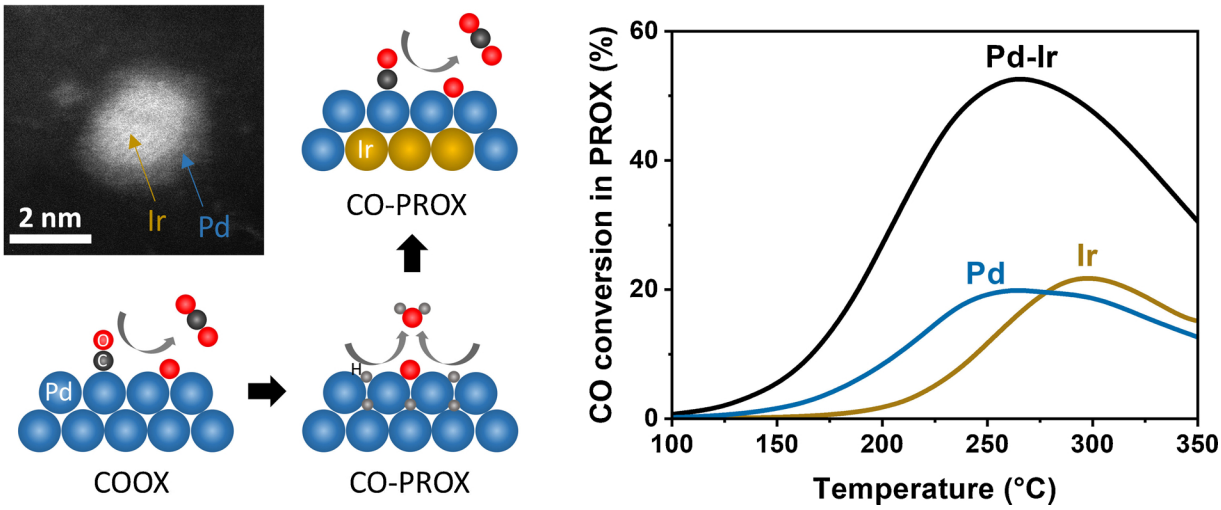

Fig. 7. Illustration of Pd hydriding and alloying effects on CO oxidation during PROX. The STEM-ADF image shows an Ir@Pd core-shell nanoparticle supported on carbon. The graph plots CO conversion vs temperature during CO-PROX reaction ($CO:O_2:H_2:He$ = 2:2:48:48 %) over Pd, Ir, and Pd-Ir NPs supported on amorphous silica-alumina.
Adapted from Ref. [165].

environment has been demonstrated for Au-Rh NPs supported on rutile titania nanorods heated to 350 °C under hydrogen [130]: whereas the Rh@Au core-shell configuration is favored in the unsupported state owing to the positive Au-Rh mixing enthalpy and the lower surface energy of Au, the supported NPs adopt a segregated Janus structure with the Rh side located at the interface between Au and TiO_2 [85,130,193,194]. This Au/Rh/TiO_2 stacking is driven by the stronger affinity of Rh with TiO_2 as compared to Au. By stabilizing the entire structure, such a segregation of Rh at the interface provides the NPs with a high resistance to sintering, as also shown for Pd-Ir/TiO_2 [163], Au-Ir/TiO_2 [195], and Cu-Ni/TiO_2 [196]. Noticeably, both Cu-Ni/TiO_2 [196] and Au-Rh/TiO_2 [104] exhibit synergistic effects for the hydrodeoxygenation of biomass derivatives.

Using NAPXPS to analyze the structure of Pd-Rh NPs under ethanol steam reforming conditions, Llorca and coworkers have shown that the ceria support enhances the reactivity of the particles while limiting their surface rearrangement [197]. Furthermore, the support morphology strongly influences the NP reorganization under reaction conditions, and thereby the catalytic performance. Whereas on CeO_2 nanocubes both Rh and Pd strongly oxidize and ethanol mainly dehydrogenates into H_2 and acetaldehyde, on CeO_2 nanorods the metals are less oxidized, the NP surface is enriched in Pd, and H_2 is the main product (Fig. 8) [198].

3.2.3. *Strong metal-support interaction*

An even more dramatic effect of the reaction medium on supported NPs is the well-known "strong metal-support interaction" (SMSI) effect, when atoms from the support diffuse onto the NPs and encapsulate them, generally leading to inhibition of chemisorption and deactivation of the catalyst. This process was first reported by Tauster et al. in 1978 for noble metals supported on reducible oxides such as TiO_2, V_2O_3 and Nb_2O_5 upon reducing treatment at around 500 °C [199,200]. The SMSI effect was later observed for many metal/oxide catalytic systems [26,72,188,201–203]. For a given oxide support, the extent of encapsulation depends on the phase and the texture of the oxide [183].

The SMSI state would form after partial reduction of the support and migration of the resulting suboxide onto the NPs. For example, encapsulation of Au NPs with TiO_x, along with negative charging of Au, was observed upon reducing treatment of Au/TiO_2 [204]. In contrast, oxygen thermal treatments appeared to trigger SMSI with positive Au charging in the cases of Au NPs supported on ZnO nanorods [205] or on phosphate supports [206]. Hydrogen thermal treatments reversed the

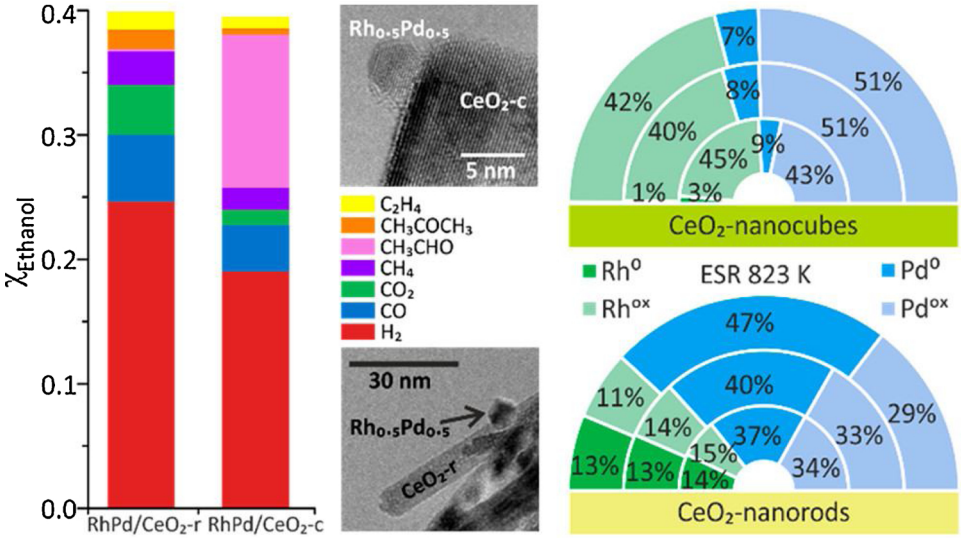

Fig. 8. Illustration of the differences in catalytic selectivities (left) between Rh-Pd NPs supported on ceria nanocubes and ceria nanorods under ethanol steam reforming conditions. TEM images of the two catalysts are displayed. Reprinted with permission from Ref [198]. Copyright 2019 American Chemical Society.

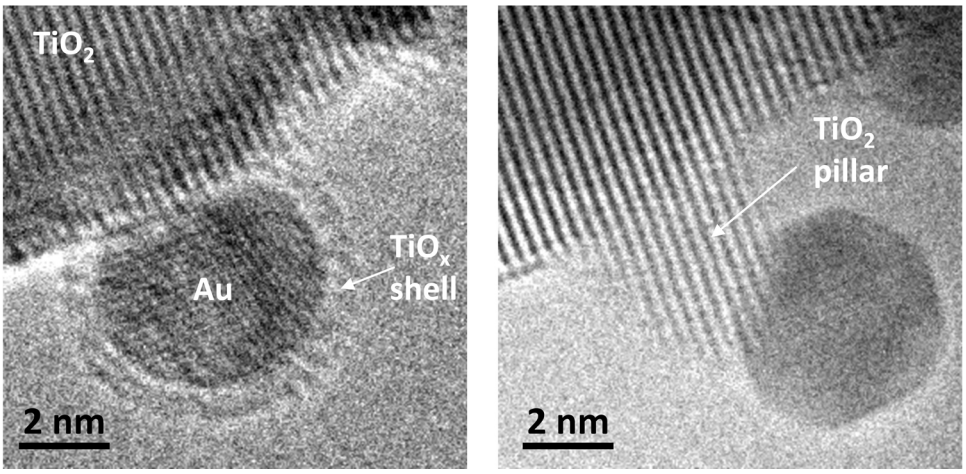

Fig. 9. Aberration-corrected ETEM images (FEI Titan ETEM G2 300 kV), recorded under 0.5 mbar of atmospheric air at 300 °C, showing a rutile TiO_2-supported Au NP encapsulated in a Ti oxide shell (left), and the same NP extracted from the shell with the formation of a rutile TiO_2 "nanopillar" (right). The extracted state was generated by condensing the TEM electron beam.

processes.

A fine tuning of the SMSI effect through suitable redox treatments can enhance the catalytic performances, as in the examples of H_2O_2 synthesis over Pd-Sn/TiO_2 nanocatalysts [207], and Fisher-Tropsch synthesis over Co NPs supported on TiO_2 or Nb_2O_5 [208].

Beyond the classical encapsulation described above, Matsubu et al. have demonstrated another type of SMSI for Rh NPs supported on TiO_2 or Nb_2O_5 under CO_2-H_2 conditions [209]. The migration of the sub-oxide would here be driven by the strong adsorption of HCO_x species and lead, unlike the usual SMSI effect, to a stable amorphous shell permeable to reactants. With respect to bare Rh, this adsorbate-mediated SMSI causes a switch of selectivity from CH_4 to CO.

In an attempt to generate and visualize the SMSI state, we performed ETEM experiments on colloidal Au and Au-Rh NPs immobilized on rutile TiO_2 nanorods [130] under air, O_2, or H_2 at low pressures (< 10 mbar). Fig. 9 shows ETEM images of a gold NP anchored to TiO_2, recorded under 0.5 mbar of air at 300 °C. We observed the presence of a TiO_x encapsulation layer (left-hand-side image), and – under electron-beam assistance – its removal accompanied by the formation of a TiO_2 "nanopillar" (right-hand-side image, see also supplementary movie S2). Whereas the encapsulated Au NP is roundish, the bare one is faceted, which again illustrates the strong influence of the metal NP environment (here, a Ti oxide layer) on its morphology. In this experiment, the beam was condensed to favor the NP extraction coupled to the nanopillar formation, which were irreversible. However, similar nanopillar structures were also observed under standard imaging conditions, though only under oxidizing atmosphere (air or O_2, not H_2 or vacuum), whereas the SMSI state was detected both under oxidizing and reducing atmospheres. Although these phenomena are not well understood, our observations confronted with literature data [204,209] strongly suggest that residual adsorbed ligands (here, polyvinyl alcohol) facilitate the dynamics of metal/oxide wetting and dewetting. They also show how dramatic the electron probe influence on the observed processes can be in ETEM.[7]

3.2.4. Reactive metal-support interaction

The interplay between the metal NPs, the support and the atmosphere can also be used to prepare supported intermetallic NPs through "reactive metal-support interaction" (RMSI) [190,211,212]. A typical example is the formation of PdZn, PdGa, and PdIn intermetallic phases from Pd/ZnO, Pd/Ga_2O_3, and Pd/In_2O_3 catalysts, respectively, upon reductive thermal treatment or under reductive reaction conditions; the resulting supported nanoalloys appeared more efficient than their monometallic Pd counterparts for methanol steam reforming, methanol synthesis, or alkyne semi hydrogenation [213–222].

The RMSI strategy is not limited to oxide supports. For example, it has been employed by Li et al. for Pt NPs supported on two-dimensional carbides, Ti_3C_2 and Nb_2C MXenes, in order to respectively form Pt_3Ti and Pt_3Nb intermetallics at the benefit of the selectivity for light alkane dehydrogenation reactions [223].

3.2.5. Sintering, redispersion, exsolution

Catalyst sintering is a well-known detrimental effect in catalysis, as the loss of active surface area through NP diffusion/coalescence or – to larger extent – Ostwald ripening[8] under gaseous or liquid environment at high temperature generally results in a decrease of catalytic activity [112,224–229] (or a change in metal-acid site balance for bifunctional catalysts [230]). NP size not only affects the metal surface area but also drives the surface structure (e.g. the fraction of low-coordinated sites) [6], and thereby the catalytic performance in the case of so-called "structure-sensitive reactions" [231].

It is often possible to regenerate a catalyst through redispersion of metal NPs into smaller species, including single atoms, from the use of suitable reactive thermal treatments [25,229,232,233]. An efficient strategy for Pt redispersion in automotive exhaust ceria-based catalysts consists in an oxidative treatment at high temperature (> 400 °C) [234,235]. According to Nagai et al., who performed *operando* QXAS and ETEM experiments on Pt/$CeZrO_x$ automotive catalysts, redispersion proceeds through migration of molecular PtO_x species from the Pt nanoparticles to the support, where they strongly anchor onto Ce cations; this mechanism is much less favorable on a weakly interacting support such as alumina [235]. A subsequent reducing treatment breaks the PtO_x–Ce bonds and leads to new Pt particles, smaller and thus more active than their parents in CO oxidation. As further shown by Gänzler et al. for Pt/CeO_2/Al_2O_3 using similar techniques, a controlled reduction of the redispersed catalyst with a series of fast redox cycles (as in diesel exhaust conditions), enables a tuning of the Pt NP size and oxidation state (Fig. 10) [234]. The same group found that the CO oxidation performances were optimal for reduced NPs of 1.4 nm in size, which would maximize the Pt-ceria interface perimeter and thereby the (beneficial) low-temperature reduction of ceria through hydrogen spillover [236]. Moreover, CO appeared as a more efficient reductant than H_2.

Similarly, in the commercial Pd/LaFe(Co)O_3 "intelligent catalyst", redox cycles cause Pd incorporation as cations into the perovskite lattice (oxidation step) followed by surface segregation of Pd NPs

[7] The energy and momentum transferred to the atoms of a material exposed to an electron beam have been used e.g. to investigate single-atom dynamics by STEM [210].

[8] Growth of larger particles at the expense of smaller ones, leading to a minimization of the surface energy. In the case of nanoalloys, this process can lead to NP size-composition correlation [224].

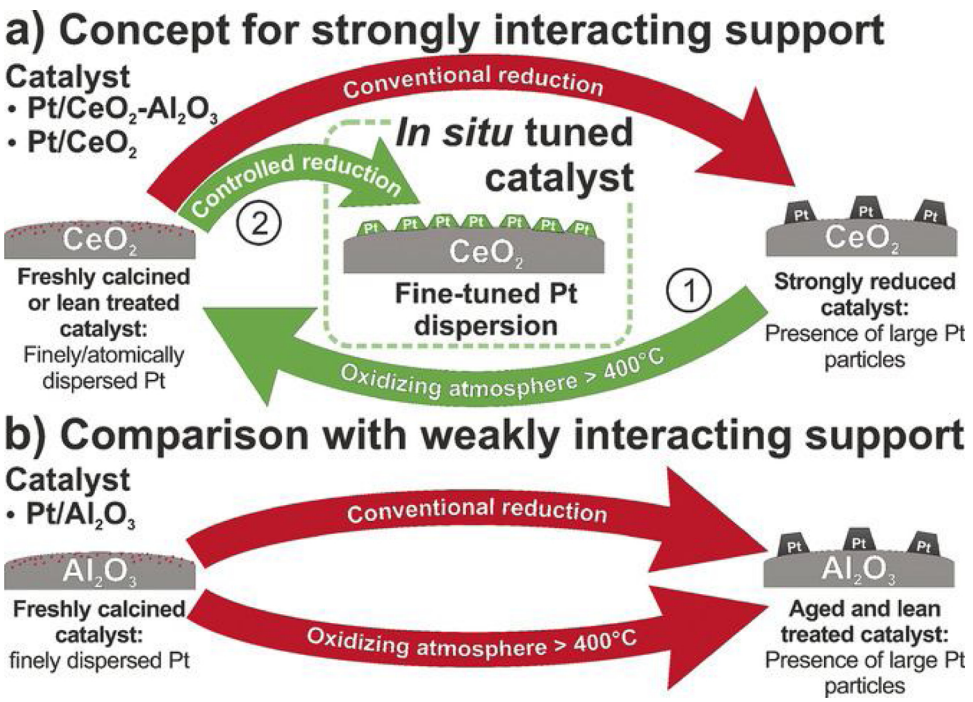

Fig. 10. a) Dynamic nature of Pt on ceria is exploited to adjust noble metal dispersion. 1) The noble metal is finely dispersed on CeO_2 during oxidative treatment by exploiting metal–support interaction with ceria. 2) Formation of slightly larger noble metal particles is initiated by the application of controlled reducing steps (for example, pulses) at a low temperature (< 400 °C). b) Redispersion step is not applicable at moderate temperatures for weakly interacting supports like Al_2O_3.
Reprinted with permission from Ref. [234]. Copyright 2017 Wiley.

(reduction step), preventing them from agglomeration during car operation [226,237,238]. The controlled reduction of perovskite oxides is also a way to grow well-defined metal or oxide NPs with enhanced catalytic properties, including resistance to coking [239,240]. Nickel NP exsolution from a $LaCaNiTiO_3$ perovskite under reducing conditions has been recently observed at atomic resolution and in real time by ETEM; such particles are socketed in, and strained by the oxide [241].

Using *in situ* TEM, Liu et al. investigated the dynamic structural transformation of subnanometric Pt species in the pores of an MCM-22 zeolite [242]. At low temperature (< 400 °C), Pt clusters tend to redisperse under oxidative atmospheres of reaction (redispersion extent: $NO + CO > NO + H_2$) but grow under reductive ones (growth extent: $CO + H_2O > CO + O_2$), while the reverse processes can be activated at higher temperatures.

Apart from oxidation and reduction treatments, the use of halogen species is also known to favor redispersion [243]. In particular, chlorine is used in industrial hydrocarbon reforming (chlorination and oxychlorination processes) to regenerate sintered Pt/Al_2O_3 catalysts. In addition, due to the low cohesion energy of rhodium and its strong affinity to CO, small supported Rh nanoparticles were shown to disintegrate into isolated organometallic $Rh^I(CO)_2$ species under several reactive conditions [4,229,233,244].

3.2.6. *Environment effects on single-atom catalysts*

Single-atom catalysis [9,245,246], or more generally catalysis by subnanometric particles showing ca. 100 % metal dispersion,[9] is a recent field of research which promises unexpected catalytic performances while saving huge amounts of rare and expensive metals. SACs most often consist of isolated metal heteroatoms anchored at the surface of a carbon-based material or a metal oxide. Although they present similarities with heterogenized homogeneous ("single-site") catalysts such as oxide-grafted metal complexes [246,248,249], in SACs the metal atom is, by design, free from organic ligands; only the solid support (or "host") is expected to stabilize it. Some authors also consider atoms of one metal diluted at the surface another metal as a subclass of SACs, namely "single-atom alloys" [250]. Also with this approach, the isolation of active centers plays a key-role in modifying the adsorptive and catalytic properties of a metal, like in the positive cases of selective styrene and acetylene hydrogenations on Pd/Cu [250] and methanol reforming on Cu/Ag [251]. In the latter system, according to DFT calculations, the isolated Cu atoms would exhibit a free atom-like electronic structure, making their bonding to adsorbates similar to that in molecular metal complexes. Single-atom alloys may include complex intermetallics such as $Al_{13}M_4$ phases, at the surface of which transition metal atoms M (Fe, Co…) were found to act as highly active and selective isolated centers for acetylene and butadiene hydrogenations [252–255].

Subnanometric metal species are inherently instable and tend to agglomerate in certain reaction conditions [116,242], making the choice of the stabilizing support critical. This is especially true for single noble-metal atoms supported on oxides under reducing conditions, as previously mentioned for Pt and Pd hosted by ceria or perovskites. In a recent work on the prototypical $Pt/\gamma\text{-}Al_2O_3$ system, we have shown using XAS, ETEM and DFT methods, that single Pt atoms (cations) are stabilized in air thanks to the formation of $Pt–O_{ads}–Al$ bridges (Fig. 4), whereas they aggregate into 0.9 nm-sized clusters under hydrogen pressure [20]. Furthermore, as shown from *operando* XAS and DRIFTS monitoring, even under oxygen-rich conditions Pt atoms gradually aggregate during heating/cooling cycles of CO oxidation (Fig. 11) [10]. In this case, metal clusters appear more active than single atoms. This is also valid for Pt/TiO_2 in photocatalytic hydrogen evolution conditions, under which single Pt atoms readily aggregate [247,256,257]. Such a dramatic sensitivity of atomic dispersion to the atmosphere is increasingly characterized by electron microscopy [234,242,258–260], and systems for which metal clusters are catalytically superior to single atoms are increasingly reported [257,258,261–264]. However, depending on the catalytic conditions and provided that the metal loading/support surface area ratio is low enough, single atoms can anchor at specific sites of the oxide support

[9] I propose to employ the term "*ultradispersion*" [247] when all the metal atoms are virtually in contact with the reactants or the support. This corresponds to a metal dispersion of 100% (*i.e.*, there are no subsurface atoms in the particle), as in the case of bilayer clusters. *Atomic dispersion* is a subgroup of ultradispersion where all the metal atoms virtually "see" both the reactants and the support (2D rafts, multimers, single atoms). *Single-atom dispersion* is itself a subcategory of atomic dispersion, as the atoms are isolated: single-atomic ⊆ atomic ⊆ ultra dispersion.

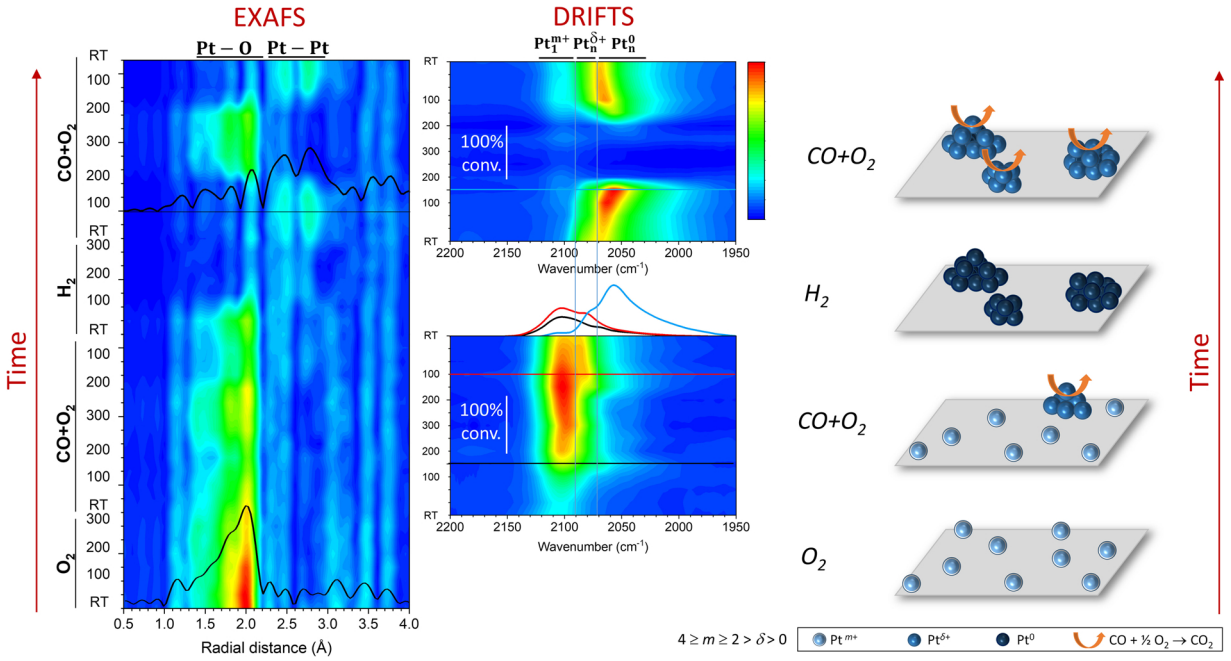

Fig. 11. Operando EXAFS and DRIFTS monitoring of 0.3 wt% Pt/γ-Al_2O_3 catalyst in CO oxidation conditions (CO:O_2 = 2:10 %), after calcination or reduction. Y-scales indicate temperatures in °C. Color Z-scales represent EXAFS FT module and IR absorbance. The picture at the right-hand side illustrates the state of the Pt species at each step.
Adapted from Ref. [10].

surface in such a way that the influence of a reducing atmosphere on their local coordination can be more subtle and avoid metal clustering [265].

It seems that carbon-based materials such as graphene and carbon nitride act as efficient stabilizing supports or hosts for single metal atoms, while preserving their catalytic ability [9,246]. There have been many demonstrations of the efficiency of such systems, especially for liquid-phase catalysis including electrocatalysis. In particular, so-called M–N–C catalysts, where M is a transition metal atom coordinated to four N atoms of an N-doped carbon in a metal–porphyrin like configuration, are frequently reported. For example, Fe–N–C has been recently shown as a highly active and stable system for CO_2 electroreduction to form CO or CH_4 [266,267].[10] Karapinar et al. have reported the selective formation of ethanol from CO_2 reduction on a Cu–N–C material [269]. However, *operando* XAS characterization suggests that, under reaction conditions, the single Cu atoms (reversibly) aggregate into subnanometric metallic clusters, which are likely to be the actual active species.

In some cases, SACs could be advantageous alternative to homogeneous catalysts: Chen et al. have reported that single Pd atoms anchored on exfoliated graphitic carbon nitride, while being stable, exhibit an adaptative coordination which facilitates the steps of Suzuki coupling catalysis [270]. Similarly, the high "fluxionality" [271] or "ductility" [118] of subnanometric clusters, which adapt their structure to the reaction medium, enables a breakup of the scaling relationships[11] that limit the possibilities of catalyst improvement [272]. This shows that the intrinsic sensitivity of ultradispersed metal species – whether single atoms or clusters – to their chemical environment can turn a weakness into a strength. More generally, beyond well-reported restructuring events such as NP morphology changes, tiny fluctuations in the catalyst surface atomic structure at the timescale of the catalytic cycle can have important consequences on the overall performance.

4. Conclusive discussion and outlook

A number of restructuring effects of the chemical environment on metal-based nanocatalysts and single-atom catalysts, in the course of their pretreatment or catalytic operation, have been reviewed. These effects have been rationalized and illustrated mostly with examples from the recent literature reporting *in situ/operando* investigations. The viewpoint of the metal particle (nanoparticle, cluster, or single atom) has been adopted. Within this approach, from the attempt to categorize dynamic environment effects, it appears that restructuring phenomena can be categorized according to the influence of the particle support (if any). The first category, in which the role of the support is not central since the effects can also be observed with unsupported particles, includes particle reshaping, metal segregation, oxidation and hydriding. The second category relates to dynamic metal-support interaction phenomena such as SMSI, RMSI and metal redispersion. The restructuring effects specific to small clusters and single atoms are necessarily related to the support, owing to its fundamental stabilizing role. A close examination of adsorbate-metal-support interaction-induced restructuring processes leads to the conclusion that they exhibit similarities and links with each other, as depicted in Fig. 12 for a metal/oxide system under oxidizing or reducing conditions.

As underlined in this minireview, in the last twenty years, the knowledge of restructuring phenomena in heterogeneous catalysis has strongly benefited from the increasing use of the *operando* methodology, combining kinetic measurements with one or more characterization techniques. In the case of ultradispersed metals such as oxide-supported noble-metal single atoms prone to destabilization, this approach has appeared crucial for determining the actual nature of active species. Moreover, aberration-corrected TEM/STEM and related techniques, possibly performed "*in situ*", nicely complement *operando* spectroscopies by offering a direct visualization of the atomic and

[10] With relatively similar coordination environment, FeN_5 centers confined in carbon nanomaterials, so-called "single-atom nanozymes", have been shown to possess high oxidase-like activity [268].

[11] Scaling relationships typically refer to the existence of linear correlations between the adsorption energies of intermediate species in a given catalytic reaction. Consequently, a more/less reactive surface will generally bind all the reactive intermediates more/less strongly without changing the energy barriers between them.

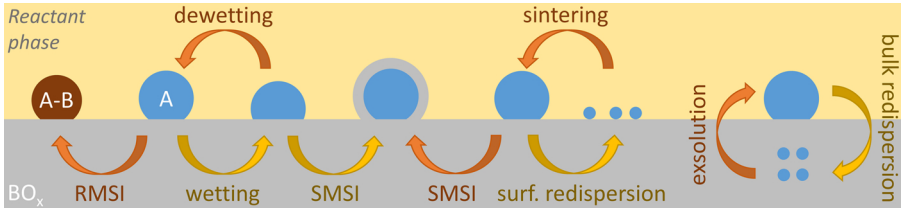

Fig. 12. Illustration of reaction medium/metal particle/oxide support interaction phenomena in heterogeneous catalysis. Large disks represent nanoparticles or clusters, while small ones represent single atoms. Orange and yellow arrows denote (most frequently) reductive and oxidative processes, respectively. SMSI and RMSI stand for strong metal-support interaction and reactive metal-support interaction, respectively.

chemical structures of nanocatalysts and SACs. Understanding how a catalyst dynamically adapts to its chemical environment is an important route toward the design of more structurally stable and poison-resistant catalysts.

In the near future, the simultaneous tracking of the catalyst structure, the surface adsorbates as well as the reactants and products, together with multiscale theoretical modeling, is expected to bring a more comprehensive knowledge of catalysis mechanisms. In addition, since most works have examined restructuring phenomena from a thermodynamic perspective (e.g. experimentally at steady state before and after modifying the reactant mixture composition, or theoretically at equilibrium), significant efforts are expected in the investigation of catalyst evolution kinetics and metastable/unstable active states. In turn, the time-resolved atomic-scale understanding of these processes is an important step toward the fine control of catalyst elaboration and the selection of pretreatment/reaction conditions. This review has provided some examples of knowledge-driven achievements, as e.g. the dynamic control of metal dispersion in car-exhaust catalysts. A more rational and predictive approach of catalysis will be highly beneficial to human kind for addressing the present and future environmental and energetic challenges.

Declaration of Competing Interest

The author declares that he has no known competing financial interests or personal relationships that could have appeared to influence the work reported in this paper.

Acknowledgements

CLYM is acknowledged for access to the Titan microscope. CNRS-IRN Nanoalloys is acknowledged for fruitful scientific discussions. I thank my colleagues from IRCELYON, my students and post-docs, and my collaborators. All of them have contributed, in one way or another, to the works reported here. I specially thank C. Chizallet and E. Gaudry for their suggestions on the manuscript; P. Andreazza, M. Bugnet, S. Loridant, F. Maillard, and C. Zlotea for their insights on X-ray scattering, electron microscopy, vibrational spectroscopy, electrocatalysis, and hydriding parts, respectively; P. Afanasiev and M. Aouine for their support in XAS and TEM experiments, respectively; F. Morfin for his constant technical and scientific help.

References

[1] G.A. Somorjai, Y. Li, Introduction to Surface Chemistry and Catalysis, 2nd ed., Wiley, Hoboken, 2010.
[2] B.M. Weckhuysen, Studying birth, life and death of catalytic solids with operando spectroscopy, Natl. Sci. Rev. 2 (2015) 147–149, https://doi.org/10.1093/nsr/nwv020.
[3] A. Chakrabarti, M.E. Ford, D. Gregory, R. Hu, C.J. Keturakis, S. Lwin, Y. Tang, Z. Yang, M. Zhu, M.A. Bañares, I.E. Wachs, A decade+ of operando spectroscopy studies, Catal. Today 283 (2017) 27–53, https://doi.org/10.1016/j.cattod.2016.12.012.
[4] K.F. Kalz, R. Kraehnert, M. Dvoyashkin, R. Dittmeyer, R. Gläser, U. Krewer, K. Reuter, J.-D. Grunwaldt, Future challenges in heterogeneous catalysis: understanding catalysts under dynamic reaction conditions, ChemCatChem 9 (2017) 17–29, https://doi.org/10.1002/cctc.201600996.
[5] A. Bergmann, B. Roldan Cuenya, Operando insights into nanoparticle transformations during catalysis, ACS Catal. 9 (2019) 10020–10043, https://doi.org/10.1021/acscatal.9b01831.
[6] L. Piccolo, Surface studies of catalysis by metals: nanosize and alloying effects, in: D. Alloyeau, C. Mottet, C. Ricolleau (Eds.), Nanoalloys: Synthesis, Structure and Properties, Springer, London, 2012, pp. 369–404, , https://doi.org/10.1007/978-1-4471-4014-6_11.
[7] Y. Dai, Y. Wang, B. Liu, Y. Yang, Metallic nanocatalysis: an accelerating seamless integration with nanotechnology, Small 11 (2015) 268–289, https://doi.org/10.1002/smll.201400847.
[8] L. Liu, A. Corma, Metal catalysts for heterogeneous catalysis: from single atoms to nanoclusters and nanoparticles, Chem. Rev. 118 (2018) 4981–5079, https://doi.org/10.1021/acs.chemrev.7b00776.
[9] A. Wang, J. Li, T. Zhang, Heterogeneous single-atom catalysis, Nat. Rev. Chem. 2 (2018) 65–81, https://doi.org/10.1038/s41570-018-0010-1.
[10] C. Dessal, T. Len, F. Morfin, J.-L. Rousset, M. Aouine, P. Afanasiev, L. Piccolo, Dynamics of single Pt atoms on alumina during CO oxidation monitored by operando X-ray and infrared spectroscopies, ACS Catal. 9 (2019) 5752–5759, https://doi.org/10.1021/acscatal.9b00903.
[11] N. Daelman, M. Capdevila-Cortada, N. López, Dynamic charge and oxidation state of Pt/CeO_2 single-atom catalysts, Nat. Mater. 18 (2019) 1215–1221, https://doi.org/10.1038/s41563-019-0444-y.
[12] M.A. Bañares, M.O. Guerrero-Pérez, J.L.G. Fierro, G.G. Cortez, Raman spectroscopy during catalytic operations with on-line activity measurement (operando spectroscopy): a method for understanding the active centres of cations supported on porous materials, J. Mater. Chem. 12 (2002) 3337–3342, https://doi.org/10.1039/B204494C.
[13] B.M. Weckhuysen, Operando spectroscopy: fundamental and technical aspects of spectroscopy of catalysts under working conditions, Phys. Chem. Chem. Phys. 5 (2003), https://doi.org/10.1039/B309654H vi–vi.
[14] M.A. Bañares, Operando methodology: combination of in situ spectroscopy and simultaneous activity measurements under catalytic reaction conditions, Catal. Today 100 (2005) 71–77, https://doi.org/10.1016/j.cattod.2004.12.017.
[15] J.W. Niemantsverdriet, Spectroscopy in Catalysis: An Introduction, 3rd edition, Wiley-VCH, Weinheim, Chichester, 2007.
[16] I.L.C. Buurmans, B.M. Weckhuysen, Heterogeneities of individual catalyst particles in space and time as monitored by spectroscopy, Nat. Chem. 4 (2012) 873–886, https://doi.org/10.1038/nchem.1478.
[17] J.A. Rodriguez, J.C. Hanson, P.J. Chupas (Eds.), In-Situ Characterization of Heterogeneous Catalysts, Wiley, Hoboken, New Jersey, 2013.
[18] J. Frenken, I. Groot, Operando Research in Heterogeneous Catalysis, Springer International Publishing AG, New York, NY, 2017.
[19] A.D. Handoko, F. Wei, Jenndy, B.S. Yeo, Z.W. Seh, Understanding heterogeneous electrocatalytic carbon dioxide reduction through operando techniques, Nat. Catal. 1 (2018) 922–934, https://doi.org/10.1038/s41929-018-0182-6.
[20] C. Dessal, A. Sangnier, C. Chizallet, C. Dujardin, F. Morfin, J.-L. Rousset, M. Aouine, M. Bugnet, P. Afanasiev, L. Piccolo, Atmosphere-dependent stability and mobility of catalytic Pt single atoms and clusters on γ-Al_2O_3, Nanoscale 11 (2019) 6897–6904, https://doi.org/10.1039/C9NR01641D.
[21] T.-S. Nguyen, G. Postole, S. Loridant, F. Bosselet, L. Burel, M. Aouine, L. Massin, F. Morfin, P. Gélin, L. Piccolo, Ultrastable iridium-ceria nanopowders synthesized in one step by solution combustion for catalytic hydrogen production, J. Mater. Chem. A 2 (2014) 19822–19832, https://doi.org/10.1039/c4ta04820b.
[22] I.E. Wachs, C.A. Roberts, Monitoring surface metal oxide catalytic active sites with Raman spectroscopy, Chem. Soc. Rev. 39 (2010) 5002–5017, https://doi.org/10.1039/C0CS00145G.
[23] M. Daniel, S. Loridant, Probing reoxidation sites by in situ Raman spectroscopy: differences between reduced CeO_2 and Pt/CeO_2, J. Raman Spectrosc. 43 (2012) 1312–1319, https://doi.org/10.1002/jrs.4030.
[24] F. Morfin, T.-S. Nguyen, J.-L. Rousset, L. Piccolo, Synergy between hydrogen and ceria in Pt-catalyzed CO oxidation: an investigation on Pt–CeO_2 catalysts synthesized by solution combustion, Appl. Catal. B 197 (2016) 2–13, https://doi.org/10.1016/j.apcatb.2016.01.056.
[25] A.R. Passos, C.L. Fontaine, L. Martins, S.H. Pulcinelli, C.V. Santilli, V. Briois, Operando XAS/Raman/MS monitoring of ethanol steam reforming reaction–regeneration cycles, Catal. Sci. Technol. 8 (2018) 6297–6301, https://doi.org/10.1039/C8CY01596A.
[26] M. Zhu, P. Tian, R. Kurtz, T. Lunkenbein, J. Xu, R. Schlögl, I.E. Wachs, Y.-F. Han,

Strong metal–support interactions between copper and iron oxide during the high-temperature water-gas shift reaction, Angew. Chem. Int. Ed. 58 (2019) 9083–9087, https://doi.org/10.1002/anie.201903298.
[27] S. Loridant, Raman spectroscopy as a powerful tool to characterize ceria-based catalysts, Catal. Today (2020), https://doi.org/10.1016/j.cattod.2020.03.044 In press.
[28] E. Stavitski, Infrared spectroscopy on powder catalysts, In-Situ Characterization of Heterogeneous Catalysts, John Wiley & Sons, Ltd, 2013, pp. 241–265, https://doi.org/10.1002/9781118355923.
[29] E. Roze, P. Gravejat, E. Quinet, J.-L. Rousset, D. Bianchi, Impact of the reconstruction of gold particles on the heats of adsorption of linear CO species adsorbed on the Au sites of a 1% Au/Al_2O_3 catalyst, J. Phys. Chem. C 113 (2009) 1037–1045, https://doi.org/10.1021/jp8062838.
[30] F.C. Meunier, Pitfalls and benefits of in situ and operando diffuse reflectance FT-IR spectroscopy (DRIFTS) applied to catalytic reactions, React. Chem. Eng. 1 (2016) 134–141, https://doi.org/10.1039/C5RE00018A.
[31] L. Piccolo, H. Daly, A. Valcarcel, F.C. Meunier, Promotional effect of H_2 on CO oxidation over Au/TiO_2 studied by operando infrared spectroscopy, Appl. Catal. B 86 (2009) 190–195, https://doi.org/10.1016/j.apcatb.2008.08.011.
[32] A. Kaftan, F. Kollhoff, T.-S. Nguyen, L. Piccolo, M. Laurin, J. Libuda, Sensitivity of CO oxidation toward metal oxidation state in ceria-supported catalysts: an operando DRIFTS-MS study, Catal. Sci. Technol. 6 (2016) 818–828, https://doi.org/10.1039/C5CY00827A.
[33] J. Ramade, E. Cottancin, M.-A. Lebeault, C. Langlois, L. Piccolo, M. Broyer, M. Hillenkamp, J. Lermé, F. Calvo, M. Pellarin, Environmental plasmonic spectroscopy of silver–iron nanoparticles: chemical ordering under oxidizing and reducing conditions, J. Phys. Chem. C 123 (2019) 15693–15706, https://doi.org/10.1021/acs.jpcc.9b02422.
[34] E.M. Larsson, C. Langhammer, I. Zorić, B. Kasemo, Nanoplasmonic probes of catalytic reactions, Science 326 (2009) 1091–1094, https://doi.org/10.1126/science.1176593.
[35] J.F. Li, Y.F. Huang, Y. Ding, Z.L. Yang, S.B. Li, X.S. Zhou, F.R. Fan, W. Zhang, Z.Y. Zhou, D.Y. Wu, B. Ren, Z.L. Wang, Z.Q. Tian, Shell-isolated nanoparticle-enhanced Raman spectroscopy, Nature 464 (2010) 392–395, https://doi.org/10.1038/nature08907.
[36] S. Bordiga, E. Groppo, G. Agostini, J.A. van Bokhoven, C. Lamberti, Reactivity of surface species in heterogeneous catalysts probed by in situ X-ray absorption techniques, Chem. Rev. 113 (2013) 1736–1850, https://doi.org/10.1021/cr2000898.
[37] J. Timoshenko, Z. Duan, G. Henkelman, R.M. Crooks, A.I. Frenkel, Solving the structure and dynamics of metal nanoparticles by combining X-ray absorption fine structure spectroscopy and atomistic structure simulations, Annu. Rev. Anal. Chem. 12 (2019) 501–522, https://doi.org/10.1146/annurev-anchem-061318-114929.
[38] Q. Liu, Z. Zhang, Platinum single-atom catalysts: a comparative review towards effective characterization, Catal. Sci. Technol. 9 (2019) 4821–4834, https://doi.org/10.1039/C9CY01028A.
[39] P. Andreazza, Probing nanoalloy structure and morphology by X-ray scattering methods, in: D. Alloyeau, C. Mottet, C. Ricolleau (Eds.), Nanoalloys: Synthesis, Structure and Properties, Springer, London, 2012, pp. 69–112, , https://doi.org/10.1007/978-1-4471-4014-6_3.
[40] B. Ingham, X-ray scattering characterisation of nanoparticles, Crystallogr. Rev. 21 (2015) 229–303, https://doi.org/10.1080/0889311X.2015.1024114.
[41] S. Nassreddine, G. Bergeret, B. Jouguet, C. Geantet, L. Piccolo, Operando study of iridium acetylacetonate decomposition on amorphous silica-alumina for bifunctional catalyst preparation, Phys. Chem. Chem. Phys. 12 (2010) 7812–7820, https://doi.org/10.1039/b925062j.
[42] Y. Maswadeh, S. Shan, B. Prasai, Y. Zhao, Z.-H. Xie, Z. Wu, J. Luo, Y. Ren, C.-J. Zhong, V. Petkov, Charting the relationship between phase type-surface area-interactions between the constituent atoms and oxygen reduction activity of Pd–Cu nanocatalysts inside fuel cells by in operando high-energy X-ray diffraction, J. Mater. Chem. A 5 (2017) 7355–7365, https://doi.org/10.1039/C7TA00688H.
[43] T. Li, A.J. Senesi, B. Lee, Small angle X-ray scattering for nanoparticle research, Chem. Rev. 116 (2016) 11128–11180, https://doi.org/10.1021/acs.chemrev.5b00690.
[44] V. Petkov, S.D. Shastri, Element-specific structure of materials with intrinsic disorder by high-energy resonant x-ray diffraction and differential atomic pair-distribution functions: a study of PtPd nanosized catalysts, Phys. Rev. B 81 (2010) 165428, , https://doi.org/10.1103/PhysRevB.81.165428.
[45] X. Chen, J. Schröder, S. Hauschild, S. Rosenfeldt, M. Dulle, S. Förster, Simultaneous SAXS/WAXS/UV–vis study of the nucleation and growth of nanoparticles: a test of classical nucleation theory, Langmuir 31 (2015) 11678–11691, https://doi.org/10.1021/acs.langmuir.5b02759.
[46] P. Andreazza, V. Pierron-Bohnes, F. Tournus, C. Andreazza-Vignolle, V. Dupuis, Structure and order in cobalt/platinum-type nanoalloys: from thin films to supported clusters, Surf. Sci. Rep. 70 (2015) 188–258, https://doi.org/10.1016/j.surfrep.2015.02.002.
[47] P. Andreazza, H. Khelfane, O. Lyon, C. Andreazza-Vignolle, A.Y. Ramos, M. Samah, Trends in anomalous small-angle X-ray scattering in grazing incidence for supported nanoalloyed and core-shell metallic nanoparticles, Eur. Phys. J. Spec. Top. 208 (2012) 231–244, https://doi.org/10.1140/epjst/e2012-01621-4.
[48] S. Alayoglu, G.A. Somorjai, Ambient pressure X-ray photoelectron spectroscopy for probing monometallic, bimetallic and oxide-metal catalysts under reactive atmospheres and catalytic reaction conditions, Top. Catal. 59 (2016) 420–438, https://doi.org/10.1007/s11244-015-0534-2.
[49] L. Nguyen, F.F. Tao, Y. Tang, J. Dou, X.-J. Bao, Understanding catalyst surfaces during catalysis through near ambient pressure X-ray photoelectron spectroscopy, Chem. Rev. 119 (2019) 6822–6905, https://doi.org/10.1021/acs.chemrev.8b00114.
[50] L. Zhong, D. Chen, S. Zafeiratos, A mini review of in situ near-ambient pressure XPS studies on non-noble, late transition metal catalysts, Catal. Sci. Technol. 9 (2019) 3851–3867, https://doi.org/10.1039/C9CY00632J.
[51] K.A. Stoerzinger, W.T. Hong, E.J. Crumlin, H. Bluhm, Y. Shao-Horn, Insights into electrochemical reactions from ambient pressure photoelectron spectroscopy, Acc. Chem. Res. 48 (2015) 2976–2983, https://doi.org/10.1021/acs.accounts.5b00275.
[52] J.J. Velasco-Velez, V. Pfeifer, M. Hävecker, R.S. Weatherup, R. Arrigo, C.-H. Chuang, E. Stotz, G. Weinberg, M. Salmeron, R. Schlögl, A. Knop-Gericke, Photoelectron spectroscopy at the graphene–liquid interface reveals the electronic structure of an electrodeposited cobalt/graphene electrocatalyst, Angew. Chem. Int. Ed. 54 (2015) 14554–14558, https://doi.org/10.1002/anie.201506044.
[53] S. Axnanda, E.J. Crumlin, B. Mao, S. Rani, R. Chang, P.G. Karlsson, M.O.M. Edwards, M. Lundqvist, R. Moberg, P. Ross, Z. Hussain, Z. Liu, Using "tender" X-ray ambient pressure X-ray photoelectron spectroscopy as a direct probe of solid-liquid interface, Sci. Rep. 5 (2015) 9788, https://doi.org/10.1038/srep09788.
[54] P. Lettenmeier, J. Majchel, L. Wang, V.A. Saveleva, S. Zafeiratos, E.R. Savinova, J.-J. Gallet, F. Bournel, A.S. Gago, K.A. Friedrich, Highly active nano-sized iridium catalysts: synthesis and operando spectroscopy in a proton exchange membrane electrolyzer, Chem. Sci. 9 (2018) 3570–3579, https://doi.org/10.1039/C8SC00555A.
[55] A. Naitabdi, A. Boucly, F. Rochet, R. Fagiewicz, G. Olivieri, F. Bournel, R. Benbalagh, F. Sirotti, J.-J. Gallet, CO oxidation activity of Pt, Zn and ZnPt nanocatalysts: a comparative study by in situ near-ambient pressure X-ray photoelectron spectroscopy, Nanoscale 10 (2018) 6566–6580, https://doi.org/10.1039/C7NR07981H.
[56] B. Böller, K.M. Durner, J. Wintterlin, The active sites of a working Fischer–Tropsch catalyst revealed by operando scanning tunnelling microscopy, Nat Catal. 2 (2019) 1027–1034, https://doi.org/10.1038/s41929-019-0360-1.
[57] J. Gustafson, M. Shipilin, C. Zhang, A. Stierle, U. Hejral, U. Ruett, O. Gutowski, P.-A. Carlsson, M. Skoglundh, E. Lundgren, High-energy surface X-ray diffraction for fast surface structure determination, Science 343 (2014) 758–761, https://doi.org/10.1126/science.1246834.
[58] M.-C. Saint-Lager, Y. Jugnet, P. Dolle, L. Piccolo, R. Baudoing-Savois, J.-C. Bertolini, A. Bailly, O. Robach, C. Walker, S. Ferrer, Pd_8Ni_{92}(110) surface structure from surface X-ray diffraction. Surface evolution under hydrogen and butadiene reactants at elevated pressure, Surf. Sci. 587 (2005) 229–235, https://doi.org/10.1016/j.susc.2005.05.016.
[59] L. Piccolo, D. Loffreda, F.J.C.S. Aires, C. Deranlot, Y. Jugnet, P. Sautet, J.-C. Bertolini, The adsorption of CO on Au(111) at elevated pressures studied by STM, RAIRS and DFT calculations, Surf. Sci. 566–568 (2004) 995–1000, https://doi.org/10.1016/j.susc.2004.06.042.
[60] J. Dou, Z. Sun, A.A. Opalade, N. Wang, W. Fu, F. (Feng) Tao, Operando chemistry of catalyst surfaces during catalysis, Chem. Soc. Rev. 46 (2017) 2001–2027, https://doi.org/10.1039/C6CS00931J.
[61] T.W. Hansen, J.B. Wagner, Catalysts under controlled atmospheres in the transmission electron microscope, ACS Catal. 4 (2014) 1673–1685, https://doi.org/10.1021/cs401148d.
[62] D.S. Su, B. Zhang, R. Schlögl, Electron microscopy of solid catalysts—transforming from a challenge to a toolbox, Chem. Rev. 115 (2015) 2818–2882, https://doi.org/10.1021/cr500084c.
[63] P.J. Kooyman, Development of operando transmission electron microscopy, Operando Research in Heterogeneous Catalysis, Springer, Cham, 2017, pp. 111–129, https://doi.org/10.1007/978-3-319-44439-0_5.
[64] M. Bugnet, S.H. Overbury, Z.L. Wu, T. Epicier, Direct visualization and control of atomic mobility at {100} surfaces of ceria in the environmental transmission electron microscope, Nano Lett. 17 (2017) 7652–7658, https://doi.org/10.1021/acs.nanolett.7b03680.
[65] S. Koneti, L. Roiban, F. Dalmas, C. Langlois, A.-S. Gay, A. Cabiac, T. Grenier, H. Banjak, V. Maxim, T. Epicier, Fast electron tomography: applications to beam sensitive samples and in situ TEM or operando environmental TEM studies, Mater. Charact. 151 (2019) 480–495, https://doi.org/10.1016/j.matchar.2019.02.009.
[66] L. Roiban, S. Koneti, F. Morfin, T.-S. Nguyen, P. Mascunan, M. Aouine, T. Epicier, L. Piccolo, Uncovering the 3D structure of combustion-synthesized noble metal-ceria nanocatalysts, ChemCatChem 9 (2017) 4607–4613, https://doi.org/10.1002/cctc.201701474.
[67] T. Avanesian, S. Dai, M.J. Kale, G.W. Graham, X. Pan, P. Christopher, Quantitative and atomic-scale view of CO-induced Pt nanoparticle surface reconstruction at saturation coverage via DFT calculations coupled with in situ TEM and IR, J. Am. Chem. Soc. 139 (2017) 4551–4558, https://doi.org/10.1021/jacs.7b01081.
[68] A.S. Kashin, V.P. Ananikov, Monitoring chemical reactions in liquid media using electron microscopy, Nat. Rev. Chem. (2019) 1–14, https://doi.org/10.1038/s41570-019-0133-z.
[69] Z. Konuspayeva, G. Berhault, P. Afanasiev, T.-S. Nguyen, S. Giorgio, L. Piccolo, Monitoring in situ the colloidal synthesis of $AuRh/TiO_2$ selective-hydrogenation nanocatalysts, J. Mater. Chem. A 5 (2017) 17360–17367, https://doi.org/10.1039/C7TA03965D.
[70] N. Ortiz Peña, D. Ihiawakrim, M. Han, B. Lassalle-Kaiser, S. Carenco, C. Sanchez, C. Laberty-Robert, D. Portehault, O. Ersen, Morphological and structural evolution of Co_3O_4 nanoparticles revealed by in situ electrochemical transmission electron microscopy during electrocatalytic water oxidation, ACS Nano 13 (2019) 11372–11381, https://doi.org/10.1021/acsnano.9b04745.

[71] N. Hodnik, G. Dehm, K.J.J. Mayrhofer, Importance and challenges of electrochemical in situ liquid cell electron microscopy for energy conversion research, Acc. Chem. Res. 49 (2016) 2015–2022, https://doi.org/10.1021/acs.accounts.6b00330.
[72] T. Lunkenbein, J. Schumann, M. Behrens, R. Schlögl, M.G. Willinger, Formation of a ZnO overlayer in industrial Cu/ZnO/Al_2O_3 catalysts induced by strong metal-support interactions, Angew. Chem. Int. Ed. 54 (2015) 4544–4548, https://doi.org/10.1002/anie.201411581.
[73] D.J. Kelly, M. Zhou, N. Clark, M.J. Hamer, E.A. Lewis, A.M. Rakowski, S.J. Haigh, R.V. Gorbachev, Nanometer resolution elemental mapping in graphene-based TEM liquid cells, Nano Lett. 18 (2018) 1168–1174, https://doi.org/10.1021/acs.nanolett.7b04713.
[74] J.K. Nørskov, T. Bligaard, J. Rossmeisl, C.H. Christensen, Towards the computational design of solid catalysts, Nat. Chem. 1 (2009) 37–46, https://doi.org/10.1038/nchem.121.
[75] A. Bruix, J.T. Margraf, M. Andersen, K. Reuter, First-principles-based multiscale modelling of heterogeneous catalysis, Nat. Catal. 2 (2019) 659–670, https://doi.org/10.1038/s41929-019-0298-3.
[76] L. Grajciar, C.J. Heard, A.A. Bondarenko, M.V. Polynski, J. Meeprasert, E.A. Pidko, P. Nachtigall, Towards operando computational modeling in heterogeneous catalysis, Chem. Soc. Rev. 47 (2018) 8307–8348, https://doi.org/10.1039/C8CS00398J.
[77] C. Chizallet, P. Raybaud, Density functional theory simulations of complex catalytic materials in reactive environments: beyond the ideal surface at low coverage, Catal. Sci. Technol. 4 (2014) 2797–2813, https://doi.org/10.1039/C3CY00965C.
[78] T. Cheng, A. Fortunelli, W.A. Goddard, Reaction intermediates during operando electrocatalysis identified from full solvent quantum mechanics molecular dynamics, PNAS 116 (2019) 7718–7722, https://doi.org/10.1073/pnas.1821709116.
[79] A. Gorczyca, P. Raybaud, V. Moizan, Y. Joly, C. Chizallet, Atomistic models for highly-dispersed PtSn/γ-Al_2O_3 catalysts: ductility and dilution affect the affinity for hydrogen, ChemCatChem 11 (2019) 3941–3951, https://doi.org/10.1002/cctc.201900429.
[80] S. Liu, Z.-J. Zhao, C. Yang, S. Zha, K.M. Neyman, F. Studt, J. Gong, Adsorption preference determines segregation direction: a shortcut to more realistic surface models of alloy catalysts, ACS Catal. 9 (2019) 5011–5018, https://doi.org/10.1021/acscatal.9b00499.
[81] B. Hammer, J.K. Norskov, Why gold is the noblest of all the metals, Nature 376 (1995) 238, https://doi.org/10.1038/376238a0.
[82] Y. Jugnet, F.J.C.S. Aires, C. Deranlot, L. Piccolo, J.-C. Bertolini, CO chemisorption on Au(110) investigated under elevated pressures by polarized reflection absorption infrared spectroscopy and scanning tunneling microscopy, Surf. Sci. 521 (2002) L639–L644, https://doi.org/10.1016/S0039-6028(02)02295-1.
[83] D. Loffreda, L. Piccolo, P. Sautet, Surface restructuring under gas pressure from first principles: a mechanism for CO-induced removal of the Au(110)-(1×2) reconstruction, Phys. Rev. B 71 (2005), https://doi.org/10.1103/PhysRevB.71.113414 113414-1–4.
[84] Y.-G. Wang, Y. Yoon, V.-A. Glezakou, J. Li, R. Rousseau, The role of reducible oxide–metal cluster charge transfer in catalytic processes: new insights on the catalytic mechanism of CO oxidation on Au/TiO_2 from ab initio molecular dynamics, J. Am. Chem. Soc. 135 (2013) 10673–10683, https://doi.org/10.1021/ja402063v.
[85] I. Demiroglu, Z.Y. Li, L. Piccolo, R.L. Johnston, A DFT study of molecular adsorption on Au–Rh nanoalloys, Catal. Sci. Technol. 6 (2016) 6916–6931, https://doi.org/10.1039/C6CY01107A.
[86] Y.-G. Wang, D. Mei, V.-A. Glezakou, J. Li, R. Rousseau, Dynamic formation of single-atom catalytic active sites on ceria-supported gold nanoparticles, Nat. Commun. 6 (2015) 6511, https://doi.org/10.1038/ncomms7511.
[87] Y.-G. Wang, D.C. Cantu, M.-S. Lee, J. Li, V.-A. Glezakou, R. Rousseau, CO oxidation on Au/TiO_2: condition-dependent active sites and mechanistic pathways, J. Am. Chem. Soc. 138 (2016) 10467–10476, https://doi.org/10.1021/jacs.6b04187.
[88] F. Tao, S. Dag, L.-W. Wang, Z. Liu, D.R. Butcher, M. Salmeron, G.A. Somorjai, Restructuring of hex-Pt(100) under CO gas environments: formation of 2-D nanoclusters, Nano Lett. 9 (2009) 2167–2171, https://doi.org/10.1021/nl900809u.
[89] B.L.M. Hendriksen, J.W.M. Frenken, CO oxidation on Pt(110): scanning tunneling microscopy inside a high-pressure flow reactor, Phys. Rev. Lett. 89 (2002), https://doi.org/10.1103/PhysRevLett.89.046101 046101-1–4.
[90] P.L. Hansen, J.B. Wagner, S. Helveg, J.R. Rostrup-Nielsen, B.S. Clausen, H. Topsøe, Atom-resolved imaging of dynamic shape changes in supported copper nanocrystals, Science 295 (2002) 2053–2055, https://doi.org/10.1126/science.1069325.
[91] S. Giorgio, M. Cabié, C.R. Henry, Dynamic observations of Au catalysts by environmental electron microscopy, Gold Bull. 41 (2008) 167–173, https://doi.org/10.1007/BF03216594.
[92] T. Uchiyama, H. Yoshida, Y. Kuwauchi, S. Ichikawa, S. Shimada, M. Haruta, S. Takeda, Systematic morphology changes of gold nanoparticles supported on CeO_2 during CO oxidation, Angew. Chem. Int. Ed. 50 (2011) 10157–10160, https://doi.org/10.1002/anie.201102487.
[93] Y. Jiang, H. Li, Z. Wu, W. Ye, H. Zhang, Y. Wang, C. Sun, Z. Zhang, In situ observation of hydrogen-induced surface faceting for palladium–copper nanocrystals at atmospheric pressure, Angew. Chem. Int. Ed. 55 (2016) 12427–12430, https://doi.org/10.1002/anie.201605956.
[94] A. Chmielewski, J. Meng, B. Zhu, Y. Gao, H. Guesmi, H. Prunier, D. Alloyeau, G. Wang, C. Louis, L. Delannoy, P. Afanasiev, C. Ricolleau, J. Nelayah, Reshaping dynamics of gold nanoparticles under H_2 and O_2 at atmospheric pressure, ACS Nano 13 (2019) 2024–2033, https://doi.org/10.1021/acsnano.8b08530.
[95] B. Zhu, J. Meng, W. Yuan, X. Zhang, H. Yang, Y. Wang, Y. Gao, Reshaping of metal nanoparticles under reaction conditions, Angew. Chem. Int. Ed. 59 (2020) 2171–2180, https://doi.org/10.1002/anie.201906799.
[96] M. Duan, J. Yu, J. Meng, B. Zhu, Y. Wang, Y. Gao, Reconstruction of supported metal nanoparticles in reaction conditions, Angew. Chem. Int. Ed. 57 (2018) 6464–6469, https://doi.org/10.1002/anie.201800925.
[97] L. Piccolo, C.R. Henry, NO-CO reaction kinetics on Pd/MgO model catalysts: morphology and support effects, J. Mol. Catal. A 167 (2001) 181–190, https://doi.org/10.1016/S1381-1169(00)00505-7.
[98] L. Piccolo, A. Valcarcel, M. Bausach, C. Thomazeau, D. Uzio, G. Berhault, Tuning the shape of nanoparticles to control their catalytic properties: selective hydrogenation of 1,3-butadiene on Pd/Al_2O_3, Phys. Chem. Chem. Phys. 10 (2008) 5504–5506, https://doi.org/10.1039/b809651a.
[99] J. Martins, N. Batail, S. Silva, S. Rafik-Clement, A. Chaumonnot, D. Uzio, T.-S. Nguyen, L. Piccolo, Improving the catalytic performances of metal nanoparticles by combining shape control and encapsulation, Appl. Catal. A 504 (2015) 504–508, https://doi.org/10.1016/j.apcata.2014.11.034.
[100] R. Imbihl, G. Ertl, Oscillatory kinetics in heterogeneous catalysis, Chem. Rev. 95 (1995) 697–733, https://doi.org/10.1021/cr00035a012.
[101] S.B. Vendelbo, C.F. Elkjær, H. Falsig, I. Puspitasari, P. Dona, L. Mele, B. Morana, B.J. Nelissen, R. van Rijn, J.F. Creemer, P.J. Kooyman, S. Helveg, Visualization of oscillatory behaviour of Pt nanoparticles catalysing CO oxidation, Nat. Mater. 13 (2014) 884–890, https://doi.org/10.1038/nmat4033.
[102] J.L. Eslava, A. Iglesias-Juez, G. Agostini, M. Fernández-García, A. Guerrero-Ruiz, I. Rodríguez-Ramos, Time-resolved XAS investigation of the local environment and evolution of oxidation states of a Fischer–Tropsch Ru–Cs/C catalyst, ACS Catal. 6 (2016) 1437–1445, https://doi.org/10.1021/acscatal.5b02489.
[103] M. Azar, V. Caps, F. Morfin, J.-L. Rousset, A. Piednoir, J.-C. Bertolini, L. Piccolo, Insights into activation, deactivation and hydrogen-induced promotion of a Au/TiO_2 reference catalyst in CO oxidation, J. Catal. 239 (2006) 307–312, https://doi.org/10.1016/j.jcat.2006.02.012.
[104] T.-S. Nguyen, D. Laurenti, P. Afanasiev, Z. Konuspayeva, L. Piccolo, Titania-supported gold-based nanoparticles efficiently catalyze the hydrodeoxygenation of guaiacol, J. Catal. 344 (2016) 136–140, https://doi.org/10.1016/j.jcat.2016.09.016.
[105] F. Baletto, R. Ferrando, A. Fortunelli, F. Montalenti, C. Mottet, Crossover among structural motifs in transition and noble-metal clusters, J. Chem. Phys. 116 (2002) 3856–3863, https://doi.org/10.1063/1.1448484.
[106] C. Mottet, J. Goniakowski, F. Baletto, R. Ferrando, G. Treglia, Modeling free and supported metallic nanoclusters: structure and dynamics, Phase Transitions 77 (2004) 101–113, https://doi.org/10.1080/1411590310001622473.
[107] J. Magnus Rahm, P. Erhart, Beyond magic numbers: atomic scale equilibrium nanoparticle shapes for any size, Nano Lett. 17 (2017) 5775–5781, https://doi.org/10.1021/acs.nanolett.7b02761.
[108] M. Pellarin, B. Baguenard, J.L. Vialle, J. Lermé, M. Broyer, J. Miller, A. Perez, Evidence for icosahedral atomic shell structure in nickel and cobalt clusters. Comparison with iron clusters, Chem. Phys. Lett. 217 (1994) 349–356, https://doi.org/10.1016/0009-2614(93)E1474-U.
[109] D. Reinhard, B.D. Hall, P. Berthoud, S. Valkealahti, R. Monot, Size-dependent icosahedral-to-fcc structure change confirmed in unsupported nanometer-sized copper clusters, Phys. Rev. Lett. 79 (1997) 1459–1462, https://doi.org/10.1103/PhysRevLett.79.1459.
[110] M. Vaarkamp, J.T. Miller, F.S. Modica, D.C. Koningsberger, On the relation between particle morphology, structure of the metal-support interface, and catalytic properties of Pt/γ-Al_2O_3, J. Catal. 163 (1996) 294–305, https://doi.org/10.1006/jcat.1996.0330.
[111] C. Mager-Maury, G. Bonnard, C. Chizallet, P. Sautet, P. Raybaud, H_2-induced reconstruction of supported Pt clusters: metal–support interaction versus surface hydride, ChemCatChem 3 (2011) 200–207, https://doi.org/10.1002/cctc.201000324.
[112] J. Matos, L.K. Ono, F. Behafarid, J.R. Croy, S. Mostafa, A.T. DeLaRiva, A.K. Datye, A.I. Frenkel, B. Roldan Cuenya, In situ coarsening study of inverse micelle-prepared Pt nanoparticles supported on γ-Al_2O_3: pretreatment and environmental effects, Phys. Chem. Chem. Phys. 14 (2012) 11457–11467, https://doi.org/10.1039/C2CP41339F.
[113] A.I. Frenkel, M.W. Small, J.G. Smith, R.G. Nuzzo, K.O. Kvashnina, M. Tromp, An in situ study of bond strains in 1 nm Pt catalysts and their sensitivities to cluster–support and cluster–adsorbate interactions, J. Phys. Chem. C 117 (2013) 23286–23294, https://doi.org/10.1021/jp4062658.
[114] H. Mistry, F. Behafarid, S.R. Bare, B. Roldan Cuenya, Pressure-dependent effect of hydrogen adsorption on structural and electronic properties of Pt/γ-Al_2O_3 nanoparticles, ChemCatChem 6 (2014) 348–352, https://doi.org/10.1002/cctc.201300783.
[115] A. Gorczyca, V. Moizan, C. Chizallet, O. Proux, W. Del Net, E. Lahera, J.-L. Hazemann, P. Raybaud, Y. Joly, Monitoring morphology and hydrogen coverage of nanometric Pt/γ-Al_2O_3 particles by in situ HERFD–XANES and quantum simulations, Angew. Chem. Int. Ed. 53 (2014) 12426–12429, https://doi.org/10.1002/anie.201403585.
[116] W. Sinkler, S.I. Sanchez, S.A. Bradley, J. Wen, B. Mishra, S.D. Kelly, S.R. Bare, Aberration-corrected transmission electron microscopy and in situ XAFS structural characterization of Pt/γ-Al_2O_3 nanoparticles, ChemCatChem 7 (2015) 3779–3787, https://doi.org/10.1002/cctc.201500784.
[117] C. Yin, F.R. Negreiros, G. Barcaro, A. Beniya, L. Sementa, E.C. Tyo, S. Bartling, K.-H. Meiwes-Broer, S. Seifert, H. Hirata, N. Isomura, S. Nigam, C. Majumder, Y. Watanabe, A. Fortunelli, S. Vajda, Alumina-supported sub-nanometer Pt_{10}

clusters: amorphization and role of the support material in a highly active CO oxidation catalyst, J. Mater. Chem. A 5 (2017) 4923–4931, https://doi.org/10.1039/C6TA10989F.
[118] W. Zhao, C. Chizallet, P. Sautet, P. Raybaud, Dehydrogenation mechanisms of methyl-cyclohexane on γ-Al_2O_3 supported Pt_{13}: impact of cluster ductility, J. Catal. 370 (2019) 118–129, https://doi.org/10.1016/j.jcat.2018.12.004.
[119] C.H. Hu, C. Chizallet, C. Mager-Maury, M. Corral-Valero, P. Sautet, H. Toulhoat, P. Raybaud, Modulation of catalyst particle structure upon support hydroxylation: ab initio insights into Pd_{13} and Pt_{13}/γ-Al_2O_3, J. Catal. 274 (2010) 99–110, https://doi.org/10.1016/j.jcat.2010.06.009.
[120] F. Negreiros, L. Sementa, G. Barcaro, I. Fechete, L. Piccolo, A. Fortunelli, Reactivity and catalysis by nanoalloys, in: F. Calvo (Ed.), Nanoalloys: From Fundamentals to Emergent Applications, 2nd Ed., Elsevier, 2020, pp. 267–333, , https://doi.org/10.1016/B978-0-12-819847-6.00014-0.
[121] H. Fang, J. Yang, M. Wen, Q. Wu, Nanoalloy materials for chemical catalysis, Adv. Mater. 30 (2018) 1705698, , https://doi.org/10.1002/adma.201705698.
[122] C. Louis, L. Delannoy, Chapter one - selective hydrogenation of polyunsaturated hydrocarbons and unsaturated aldehydes over bimetallic catalysts, Advances in Catalysis, Academic Press, 2019, pp. 1–88, https://doi.org/10.1016/bs.acat.2019.08.002.
[123] R. Ferrando, J. Jellinek, R.L. Johnston, Nanoalloys: from theory to applications of alloy clusters and nanoparticles, Chem. Rev. 108 (2008) 845–910, https://doi.org/10.1021/cr040090g.
[124] D. Alloyeau, C. Mottet, C. Ricolleau (Eds.), Nanoalloys: Synthesis, Structure and Properties, Springer-Verlag, London, 2012, , https://doi.org/10.1007/978-1-4471-4014-6.
[125] F. Morfin, L. Piccolo, A versatile elevated-pressure reactor combined with an ultrahigh vacuum surface setup for efficient testing of model and powder catalysts under clean gas-phase conditions, Rev. Sci. Instrum. 84 (2013) 094101, , https://doi.org/10.1063/1.4818669.
[126] L. Piccolo, A. Piednoir, J.-C. Bertolini, Pd–Au single-crystal surfaces: segregation properties and catalytic activity in the selective hydrogenation of 1,3-butadiene, Surf. Sci. 592 (2005) 169–181, https://doi.org/10.1016/j.susc.2005.07.005.
[127] F. Tao, M.E. Grass, Y. Zhang, D.R. Butcher, J.R. Renzas, Z. Liu, J.Y. Chung, B.S. Mun, M. Salmeron, G.A. Somorjai, Reaction-driven restructuring of Rh-Pd and Pt-Pd core-shell nanoparticles, Science 322 (2008) 932–934, https://doi.org/10.1126/science.1164170.
[128] S. Dai, Y. Hou, M. Onoue, S. Zhang, W. Gao, X. Yan, G.W. Graham, R. Wu, X. Pan, Revealing surface elemental composition and dynamic processes involved in facet-dependent oxidation of Pt_3Co nanoparticles via in situ transmission electron microscopy, Nano Lett. 17 (2017) 4683–4688, https://doi.org/10.1021/acs.nanolett.7b01325.
[129] B. Zhu, G. Thrimurthulu, L. Delannoy, C. Louis, C. Mottet, J. Creuze, B. Legrand, H. Guesmi, Evidence of Pd segregation and stabilization at edges of AuPd nanoclusters in the presence of CO: a combined DFT and DRIFTS study, J. Catal. 308 (2013) 272–281, https://doi.org/10.1016/j.jcat.2013.08.022.
[130] Z. Konuspayeva, P. Afanasiev, T.-S. Nguyen, L. Di Felice, F. Morfin, N.-T. Nguyen, J. Nelayah, C. Ricolleau, Z.Y. Li, J. Yuan, G. Berhault, L. Piccolo, Au–Rh and Au–Pd nanocatalysts supported on rutile titania nanorods: structure and chemical stability, Phys. Chem. Chem. Phys. 17 (2015) 28112–28120, https://doi.org/10.1039/C5CP00249D.
[131] B. Mutz, H.W.P. Carvalho, S. Mangold, W. Kleist, J.-D. Grunwaldt, Methanation of CO_2: structural response of a Ni-based catalyst under fluctuating reaction conditions unraveled by operando spectroscopy, J. Catal. 327 (2015) 48–53, https://doi.org/10.1016/j.jcat.2015.04.006.
[132] F. Gao, S. McClure, M. Chen, D.W. Goodman, Comment on “Catalytic activity of the Rh surface oxide: CO oxidation over Rh(111) under realistic conditions”, J. Phys. Chem. C 114 (2010) 22369–22371, https://doi.org/10.1021/jp106796e.
[133] M.A. van Spronsen, J.W.M. Frenken, I.M.N. Groot, Surface science under reaction conditions: CO oxidation on Pt and Pd model catalysts, Chem. Soc. Rev. 46 (2017) 4347–4374, https://doi.org/10.1039/C7CS00045F.
[134] J. Gustafson, O. Balmes, C. Zhang, M. Shipilin, A. Schaefer, B. Hagman, L.R. Merte, N.M. Martin, P.-A. Carlsson, M. Jankowski, E.J. Crumlin, E. Lundgren, The role of oxides in catalytic CO oxidation over rhodium and palladium, ACS Catal. 8 (2018) 4438–4445, https://doi.org/10.1021/acscatal.8b00498.
[135] B.D. Anderson, J.B. Tracy, Nanoparticle conversion chemistry: kirkendall effect, galvanic exchange, and anion exchange, Nanoscale 6 (2014) 12195–12216, https://doi.org/10.1039/C4NR02025A.
[136] S. Jana, J.W. Chang, R.M. Rioux, Synthesis and modeling of hollow intermetallic Ni–Zn nanoparticles formed by the kirkendall effect, Nano Lett. 13 (2013) 3618–3625, https://doi.org/10.1021/nl401467r.
[137] L. Zou, J. Li, D. Zakharov, E.A. Stach, G. Zhou, In situ atomic-scale imaging of the metal/oxide interfacial transformation, Nat. Commun. 8 (2017) 307, https://doi.org/10.1038/s41467-017-00371-4.
[138] J. Ramade, C. Langlois, M. Pellarin, L. Piccolo, M.-A. Lebeault, T. Epicier, M. Aouine, E. Cottancin, Tracking the restructuring of oxidized silver-indium nanoparticles under a reducing atmosphere by environmental HRTEM, Nanoscale 9 (2017) 13563–13574, https://doi.org/10.1039/C7NR02986A.
[139] A. Moscu, C. Theodoridi, L. Cardenas, C. Thieuleux, D. Motta-Meira, G. Agostini, Y. Schuurman, F. Meunier, CO dissociation on Pt-Sn nanoparticles triggers Sn oxidation and alloy segregation, J. Catal. 359 (2018) 76–81, https://doi.org/10.1016/j.jcat.2017.12.035.
[140] D. Teschner, E. Vass, M. Hävecker, S. Zafeiratos, P. Schnörch, H. Sauer, A. Knop-Gericke, R. Schlögl, M. Chamam, A. Wootsch, A.S. Canning, J.J. Gamman, S.D. Jackson, J. McGregor, L.F. Gladden, Alkyne hydrogenation over Pd catalysts: a new paradigm, J. Catal. 242 (2006) 26–37, https://doi.org/10.1016/j.jcat.2006.05.030.
[141] D. Teschner, J. Borsodi, A. Wootsch, Z. Revay, M. Havecker, A. Knop-Gericke, S.D. Jackson, R. Schlogl, The roles of subsurface carbon and hydrogen in palladium-catalyzed alkyne hydrogenation, Science 320 (2008) 86–89, https://doi.org/10.1126/science.1155200.
[142] M. Armbrüster, M. Behrens, F. Cinquini, K. Föttinger, Y. Grin, A. Haghofer, B. Klötzer, A. Knop-Gericke, H. Lorenz, A. Ota, S. Penner, J. Prinz, C. Rameshan, Z. Révay, D. Rosenthal, G. Rupprechter, P. Sautet, R. Schlögl, L. Shao, L. Szentmiklósi, D. Teschner, D. Torres, R. Wagner, R. Widmer, G. Wowsnick, How to control the selectivity of palladium-based catalysts in hydrogenation reactions: the role of subsurface chemistry, ChemCatChem 4 (2012) 1048–1063, https://doi.org/10.1002/cctc.201200100.
[143] O. Piqué, I.Z. Koleva, F. Viñes, H.A. Aleksandrov, G.N. Vayssilov, F. Illas, Subsurface carbon: a general feature of noble metals, Angew. Chem. Int. Ed. 58 (2019) 1744–1748, https://doi.org/10.1002/anie.201813037.
[144] M. Corral Valero, P. Raybaud, Cobalt catalyzed Fischer–Tropsch synthesis: perspectives opened by first principles calculations, Catal. Lett. 143 (2013) 1–17, https://doi.org/10.1007/s10562-012-0930-1.
[145] F.D. Manchester, A. San-Martin, J.M. Pitre, The H-Pd (hydrogen-palladium) system, J. Phase Equilib. 15 (1994) 62–83, https://doi.org/10.1007/BF02667685.
[146] H. Kobayashi, H. Morita, M. Yamauchi, R. Ikeda, H. Kitagawa, Y. Kubota, K. Kato, M. Takata, Nanosize-induced hydrogen storage and capacity control in a non-hydride-forming element: rhodium, J. Am. Chem. Soc. 133 (2011) 11034–11037, https://doi.org/10.1021/ja2027772.
[147] H. Kobayashi, M. Yamauchi, H. Kitagawa, Finding hydrogen-storage capability in iridium induced by the nanosize effect, J. Am. Chem. Soc. 134 (2012) 6893–6895, https://doi.org/10.1021/ja302021d.
[148] C. Zlotea, Y. Oumellal, M. Msakni, J. Bourgon, S. Bastide, C. Cachet-Vivier, M. Latroche, First evidence of Rh nano-hydride formation at low pressure, Nano Lett. 15 (2015) 4752–4757, https://doi.org/10.1021/acs.nanolett.5b01766.
[149] C. Zlotea, L. Blondeau, A. Malouche, J. Bourgon, K. Provost, F. Morfin, L. Piccolo, Investigation of the local structure of nanosized rhodium hydride, J. Colloid Interface Sci. 524 (2018) 427–433, https://doi.org/10.1016/j.jcis.2018.04.047.
[150] F. Morfin, L. Blondeau, K. Provost, A. Malouche, L. Piccolo, C. Zlotea, Absorbed hydrogen enhances the catalytic hydrogenation activity of Rh-based nanocatalysts, Catal. Sci. Technol. 8 (2018) 2707–2715, https://doi.org/10.1039/C8CY00522B.
[151] H.A. Aleksandrov, S.M. Kozlov, S. Schauermann, G.N. Vayssilov, K.M. Neyman, How absorbed hydrogen affects the catalytic activity of transition metals, Angew. Chem. Int. Ed. 53 (2014) 13371–13375, https://doi.org/10.1002/anie.201405738.
[152] S.T. Ceyer, The unique chemistry of hydrogen beneath the surface: catalytic hydrogenation of hydrocarbons, Acc. Chem. Res. 34 (2001) 737–744, https://doi.org/10.1021/ar970030f.
[153] G. Rupprechter, G.A. Somorjai, Palladium-catalyzed hydrogenation without hydrogen: the hydrodechlorination of chlorofluorocarbons with solid state hydrogen over the palladium (111) crystal surface and its implications, Catal. Lett. 48 (1997) 17–20, https://doi.org/10.1023/A:1019079121238.
[154] A.M. Doyle, S.K. Shaikhutdinov, S.D. Jackson, H.-J. Freund, Hydrogenation on metal surfaces: why are nanoparticles more active than single crystals? Angew. Chem. Int. Ed. 42 (2003) 5240–5243, https://doi.org/10.1002/anie.200352124.
[155] M. Morkel, G. Rupprechter, H.-J. Freund, Finite size effects on supported Pd nanoparticles: interaction of hydrogen with CO and C_2H_4, Surf. Sci. 588 (2005) L209–L219, https://doi.org/10.1016/j.susc.2005.05.037.
[156] M. Wilde, K. Fukutani, W. Ludwig, B. Brandt, J.-H. Fischer, S. Schauermann, H.-J. Freund, Influence of carbon deposition on the hydrogen distribution in Pd nanoparticles and their reactivity in olefin hydrogenation, Angew. Chem. Int. Ed. 47 (2008) 9289–9293, https://doi.org/10.1002/anie.200801923.
[157] L. Piccolo, A. Piednoir, J.-C. Bertolini, Absorption and oxidation of hydrogen at Pd and Pd–Au (111) surfaces, Surf. Sci. 600 (2006) 4211–4215, https://doi.org/10.1016/j.susc.2006.01.146.
[158] A. Valcarcel, F. Morfin, L. Piccolo, Alkene hydrogenation on metal surfaces: why and when are Pd overlayers more efficient catalysts than bulk Pd? J. Catal. 263 (2009) 315–320, https://doi.org/10.1016/j.jcat.2009.02.023.
[159] A.P. Ashwell, W. Lin, M.S. Hofman, Y. Yang, M.A. Ratner, B.E. Koel, G.C. Schatz, Hydrogenation of CO to methanol on Ni(110) through subsurface hydrogen, J. Am. Chem. Soc. 139 (2017) 17582–17589, https://doi.org/10.1021/jacs.7b09914.
[160] H. Kobayashi, K. Kusada, H. Kitagawa, Creation of novel solid-solution alloy nanoparticles on the basis of density-of-states engineering by interelement fusion, Acc. Chem. Res. 48 (2015) 1551–1559, https://doi.org/10.1021/ar500413e.
[161] C. Zlotea, F. Morfin, T.-S. Nguyen, N.-T. Nguyen, J. Nelayah, C. Ricolleau, M. Latroche, L. Piccolo, Nanoalloying bulk-immiscible iridium and palladium inhibits hydride formation and promotes catalytic performances, Nanoscale 6 (2014) 9955–9959, https://doi.org/10.1039/C4NR02836H.
[162] C. Goyhenex, L. Piccolo, How the hydrogen sorption properties of palladium are modified through interaction with iridium, Phys. Chem. Chem. Phys. 19 (2017) 32451–32458, https://doi.org/10.1039/C7CP07155H.
[163] I. Demiroglu, T. Fan, Z. Li, J. Yuan, T. Liu, L. Piccolo, R.L. Johnston, Modelling free and oxide-supported nanoalloy catalysts: comparison of bulk-immiscible Pd-Ir and Au-Rh systems and influence of a TiO_2 support, Faraday Discuss. 208 (2018) 53–66, https://doi.org/10.1039/C7FD00213K.
[164] T.H. Andriamiharintsoa, A. Rakotomahevitra, L. Piccolo, C. Goyhenex, IrPd nanoalloys: simulations, from surface segregation to local electronic properties, J. Nanopart. Res. 17 (2015) 1–14, https://doi.org/10.1007/s11051-015-3020-7.
[165] F. Morfin, S. Nassreddine, J.-L. Rousset, L. Piccolo, Nanoalloying effect in the

preferential oxidation of CO over Ir–Pd catalysts, ACS Catal. 2 (2012) 2161–2168, https://doi.org/10.1021/cs3003325.
[166] O. Pozdnyakova, D. Teschner, A. Wootsch, J. Kröhnert, B. Steinhauer, H. Sauer, L. Toth, F.C. Jentoft, A. Knop-Gericke, Z. Paál, R. Schlögl, Preferential CO oxidation in hydrogen (PROX) on ceria-supported catalysts, part II: oxidation states and surface species on Pd/CeO_2 under reaction conditions, suggested reaction mechanism, J. Catal. 237 (2006) 17–28, https://doi.org/10.1016/j.jcat.2005.10.015.
[167] C. Zlotea, Y. Oumellal, K. Provost, F. Morfin, L. Piccolo, Role of hydrogen absorption in supported Pd nanocatalysts during CO-PROX: insights from operando X-ray absorption spectroscopy, Appl. Catal. B 237 (2018) 1059–1065, https://doi.org/10.1016/j.apcatb.2018.06.059.
[168] T.-S. Nguyen, F. Morfin, M. Aouine, F. Bosselet, J.-L. Rousset, L. Piccolo, Trends in the CO oxidation and PROX performances of the platinum-group metals supported on ceria, Catal. Today 253 (2015) 106–114, https://doi.org/10.1016/j.cattod.2014.12.038.
[169] H.N. Nong, T. Reier, H.-S. Oh, M. Gliech, P. Paciok, T.H.T. Vu, D. Teschner, M. Heggen, V. Petkov, R. Schlögl, T. Jones, P. Strasser, A unique oxygen ligand environment facilitates water oxidation in hole-doped $IrNiO_x$ core–shell electrocatalysts, Nat. Catal. 1 (2018) 841, https://doi.org/10.1038/s41929-018-0153-y.
[170] K.J.J. Mayrhofer, J.C. Meier, S.J. Ashton, G.K.H. Wiberg, F. Kraus, M. Hanzlik, M. Arenz, Fuel cell catalyst degradation on the nanoscale, Electrochem. Commun. 10 (2008) 1144–1147, https://doi.org/10.1016/j.elecom.2008.05.032.
[171] F. Claudel, L. Dubau, G. Berthomé, L. Sola-Hernandez, C. Beauger, L. Piccolo, F. Maillard, Degradation mechanisms of oxygen evolution reaction electrocatalysts: a combined identical-location transmission electron microscopy and X-ray photoelectron spectroscopy study, ACS Catal. 9 (2019) 4688–4698, https://doi.org/10.1021/acscatal.9b00280.
[172] T. Asset, C.J. Gommes, J. Drnec, P. Bordet, R. Chattot, I. Martens, J. Nelayah, N. Job, F. Maillard, L. Dubau, Disentangling the degradation pathways of highly defective PtNi/C nanostructures – an operando wide and small angle X-ray scattering study, ACS Catal. 9 (2019) 160–167, https://doi.org/10.1021/acscatal.8b02665.
[173] A. Pavlišič, P. Jovanovič, V.S. Šelih, M. Šala, M. Bele, G. Dražić, I. Arčon, S. Hočevar, A. Kokalj, N. Hodnik, M. Gaberšček, Atomically resolved dealloying of structurally ordered Pt nanoalloy as an oxygen reduction reaction electrocatalyst, ACS Catal. 6 (2016) 5530–5534, https://doi.org/10.1021/acscatal.6b00557.
[174] O. Kasian, S. Geiger, K.J.J. Mayrhofer, S. Cherevko, Electrochemical on-line ICP-MS in electrocatalysis research, Chem. Rec. 19 (2019) 2130–2142, https://doi.org/10.1002/tcr.201800162.
[175] M. Heinen, Y.X. Chen, Z. Jusys, R.J. Behm, In situ ATR-FTIRS coupled with on-line DEMS under controlled mass transport conditions—a novel tool for electrocatalytic reaction studies, Electrochim. Acta 52 (2007) 5634–5643, https://doi.org/10.1016/j.electacta.2007.01.055.
[176] A. Bach Delpeuch, F. Maillard, M. Chatenet, P. Soudant, C. Cremers, Ethanol oxidation reaction (EOR) investigation on Pt/C, Rh/C, and Pt-based bi- and tri-metallic electrocatalysts: a DEMS and in situ FTIR study, Appl. Catal. B 181 (2016) 672–680, https://doi.org/10.1016/j.apcatb.2015.08.041.
[177] B.K. Ly, B. Tapin, F. Epron, C. Pinel, C. Especel, M. Besson, In situ preparation of bimetallic ReO_x-Pd/TiO_2 catalysts for selective aqueous-phase hydrogenation of succinic acid to 1,4-butanediol, Catal. Today (2019), https://doi.org/10.1016/j.cattod.2019.03.024.
[178] L. Piccolo, S. Nassreddine, G. Toussaint, C. Geantet, Mechanism of tetralin ring opening and contraction over bifunctional Ir/SiO_2-Al_2O_3 catalysts, ChemSusChem 5 (2012) 1717–1723, https://doi.org/10.1002/cssc.201200080.
[179] M. Ahmadi, H. Mistry, B. Roldan Cuenya, Tailoring the catalytic properties of metal nanoparticles via support interactions, J. Phys. Chem. Lett. 7 (2016) 3519–3533, https://doi.org/10.1021/acs.jpclett.6b01198.
[180] Y. Lykhach, S.M. Kozlov, T. Skála, A. Tovt, V. Stetsovych, N. Tsud, F. Dvořák, V. Johánek, A. Neitzel, J. Mysliveček, S. Fabris, V. Matolín, K.M. Neyman, J. Libuda, Counting electrons on supported nanoparticles, Nat. Mater. 15 (2016) 284–288, https://doi.org/10.1038/nmat4500.
[181] W. Karim, C. Spreafico, A. Kleibert, J. Gobrecht, J. VandeVondele, Y. Ekinci, J.A. van Bokhoven, Catalyst support effects on hydrogen spillover, Nature 541 (2017) 68–71, https://doi.org/10.1038/nature20782.
[182] Y. Suchorski, S.M. Kozlov, I. Bespalov, M. Datler, D. Vogel, Z. Budinska, K.M. Neyman, G. Rupprechter, The role of metal/oxide interfaces for long-range metal particle activation during CO oxidation, Nat. Mater. 17 (2018) 519–522, https://doi.org/10.1038/s41563-018-0080-y.
[183] T.W. van Deelen, C.H. Mejía, K.P. de Jong, Control of metal-support interactions in heterogeneous catalysts to enhance activity and selectivity, Nat. Catal. 2 (2019) 955–970, https://doi.org/10.1038/s41929-019-0364-x.
[184] A.M. Abdel-Mageed, A. Klyushin, A. Knop-Gericke, R. Schlögl, R.J. Behm, Influence of CO on the activation, O-vacancy formation, and performance of Au/ZnO catalysts in CO_2 hydrogenation to methanol, J. Phys. Chem. Lett. 10 (2019) 3645–3653, https://doi.org/10.1021/acs.jpclett.9b00925.
[185] S.L. Hemmingson, C.T. Campbell, Trends in adhesion energies of metal nanoparticles on oxide surfaces: understanding support effects in catalysis and nanotechnology, ACS Nano 11 (2017) 1196–1203, https://doi.org/10.1021/acsnano.6b07502.
[186] E.M. Dietze, P.N. Plessow, Predicting the strength of metal–support interaction with computational descriptors for adhesion energies, J. Phys. Chem. C (2019), https://doi.org/10.1021/acs.jpcc.9b06893.
[187] N.J. O'Connor, A.S.M. Jonayat, M.J. Janik, T.P. Senftle, Interaction trends between single metal atoms and oxide supports identified with density functional theory and statistical learning, Nat. Catal. 1 (2018) 531–539, https://doi.org/10.1038/s41929-018-0094-5.
[188] I. Ro, J. Resasco, P. Christopher, Approaches for understanding and controlling interfacial effects in oxide-supported metal catalysts, ACS Catal. 8 (2018) 7368–7387, https://doi.org/10.1021/acscatal.8b02071.
[189] N.-T. Nguyen, J. Nelayah, D. Alloyeau, G. Wang, L. Piccolo, P. Afanasiev, C. Ricolleau, Thermodynamics of faceted palladium(–gold) nanoparticles supported on rutile titania nanorods studied using transmission electron microscopy, Phys. Chem. Chem. Phys. 20 (2018) 13030–13037, https://doi.org/10.1039/C8CP00737C.
[190] J.-D. Grunwaldt, A.M. Molenbroek, N.-Y. Topsøe, H. Topsøe, B.S. Clausen, In situ investigations of structural changes in Cu/ZnO catalysts, J. Catal. 194 (2000) 452–460, https://doi.org/10.1006/jcat.2000.2930.
[191] N.-T. Nguyen, J. Nelayah, P. Afanasiev, L. Piccolo, D. Alloyeau, C. Ricolleau, Structural properties of catalytically active bimetallic gold–palladium nanoparticles synthesized on rutile titania nanorods by pulsed laser deposition, Cryst. Growth Des. 18 (2018) 68–76, https://doi.org/10.1021/acs.cgd.7b00708.
[192] T.N. Pingel, M. Jørgensen, A.B. Yankovich, H. Grönbeck, E. Olsson, Influence of atomic site-specific strain on catalytic activity of supported nanoparticles, Nat. Commun. 9 (2018) 2722, https://doi.org/10.1038/s41467-018-05055-1.
[193] L. Piccolo, Z.Y. Li, I. Demiroglu, F. Moyon, Z. Konuspayeva, G. Berhault, P. Afanasiev, W. Lefebvre, J. Yuan, R.L. Johnston, Understanding and controlling the structure and segregation behaviour of AuRh nanocatalysts, Sci. Rep. 6 (2016) 35226, https://doi.org/10.1038/srep35226.
[194] I. Demiroglu, Z.Y. Li, L. Piccolo, R.L. Johnston, A DFT study of molecular adsorption on titania-supported AuRh nanoalloys, Comput. Theor. Chem. 1107 (2017) 142–151, https://doi.org/10.1016/j.comptc.2017.02.012.
[195] C.W. Han, P. Majumdar, E.E. Marinero, A. Aguilar-Tapia, R. Zanella, J. Greeley, V. Ortalan, Highly stable bimetallic AuIr/TiO_2 catalyst: physical origins of the intrinsic high stability against sintering, Nano Lett. 15 (2015) 8141–8147, https://doi.org/10.1021/acs.nanolett.5b03585.
[196] B. Seemala, C.M. Cai, C.E. Wyman, P. Christopher, Support induced control of surface composition in Cu–Ni/TiO_2 catalysts enables high yield co-conversion of HMF and furfural to methylated furans, ACS Catal. 7 (2017) 4070–4082, https://doi.org/10.1021/acscatal.7b01095.
[197] N.J. Divins, I. Angurell, C. Escudero, V. Perez-Dieste, J. Llorca, Influence of the support on surface rearrangements of bimetallic nanoparticles in real catalysts, Science 346 (2014) 620–623, https://doi.org/10.1126/science.1258106.
[198] L. Soler, A. Casanovas, J. Ryan, I. Angurell, C. Escudero, V. Pérez-Dieste, J. Llorca, Dynamic reorganization of bimetallic nanoparticles under reaction depending on the support nanoshape: the case of RhPd over ceria nanocubes and nanorods under ethanol steam reforming, ACS Catal. 9 (2019) 3641–3647, https://doi.org/10.1021/acscatal.9b00463.
[199] S.J. Tauster, S.C. Fung, R.L. Garten, Strong metal-support interactions. Group 8 noble metals supported on titanium dioxide, J. Am. Chem. Soc. 100 (1978) 170–175, https://doi.org/10.1021/ja00469a029.
[200] S.J. Tauster, S.C. Fung, Strong metal-support interactions: occurrence among the binary oxides of groups IIA-VB, J. Catal. 55 (1978) 29–35, https://doi.org/10.1016/0021-9517(78)90182-3.
[201] Q. Fu, T. Wagner, Interaction of nanostructured metal overlayers with oxide surfaces, Surf. Sci. Rep. 62 (2007) 431–498, https://doi.org/10.1016/j.surfrep.2007.07.001.
[202] M.G. Willinger, W. Zhang, O. Bondarchuk, S. Shaikhutdinov, H.-J. Freund, R. Schlögl, A case of strong metal–support interactions: combining advanced microscopy and model systems to elucidate the atomic structure of interfaces, Angew. Chem. Int. Ed. 53 (2014) 5998–6001, https://doi.org/10.1002/anie.201400290.
[203] S. Zhang, P.N. Plessow, J.J. Willis, S. Dai, M. Xu, G.W. Graham, M. Cargnello, F. Abild-Pedersen, X. Pan, Dynamical observation and detailed description of catalysts under strong metal–support interaction, Nano Lett. 16 (2016) 4528–4534, https://doi.org/10.1021/acs.nanolett.6b01769.
[204] H. Tang, Y. Su, B. Zhang, A.F. Lee, M.A. Isaacs, K. Wilson, L. Li, Y. Ren, J. Huang, M. Haruta, B. Qiao, X. Liu, C. Jin, D. Su, J. Wang, T. Zhang, Classical strong metal–support interactions between gold nanoparticles and titanium dioxide, Sci. Adv. 3 (2017) e1700231, , https://doi.org/10.1126/sciadv.1700231.
[205] X. Liu, M.-H. Liu, Y.-C. Luo, C.-Y. Mou, S.D. Lin, H. Cheng, J.-M. Chen, J.-F. Lee, T.-S. Lin, Strong metal–support interactions between gold nanoparticles and ZnO nanorods in CO oxidation, J. Am. Chem. Soc. 134 (2012) 10251–10258, https://doi.org/10.1021/ja3033235.
[206] H. Tang, J. Wei, F. Liu, B. Qiao, X. Pan, L. Li, J. Liu, J. Wang, T. Zhang, Strong metal–support interactions between gold nanoparticles and nonoxides, J. Am. Chem. Soc. 138 (2016) 56–59, https://doi.org/10.1021/jacs.5b11306.
[207] S.J. Freakley, Q. He, J.H. Harrhy, L. Lu, D.A. Crole, D.J. Morgan, E.N. Ntainjua, J.K. Edwards, A.F. Carley, A.Y. Borisevich, C.J. Kiely, G.J. Hutchings, Palladium-tin catalysts for the direct synthesis of H_2O_2 with high selectivity, Science 351 (2016) 965–968, https://doi.org/10.1126/science.aad5705.
[208] C. Hernández Mejía, T.W. van Deelen, K.P. de Jong, Activity enhancement of cobalt catalysts by tuning metal-support interactions, Nat. Commun. 9 (2018) 1–8, https://doi.org/10.1038/s41467-018-06903-w.
[209] J.C. Matsubu, S. Zhang, L. DeRita, N.S. Marinkovic, J.G. Chen, G.W. Graham, X. Pan, P. Christopher, Adsorbate-mediated strong metal–support interactions in oxide-supported Rh catalysts, Nat. Chem. 9 (2016) 120–127, https://doi.org/10.1038/nchem.2607.
[210] R. Mishra, R. Ishikawa, A.R. Lupini, S.J. Pennycook, Single-atom dynamics in scanning transmission electron microscopy, MRS Bull. 42 (2017) 644–652, https://doi.org/10.1557/mrs.2017.187.
[211] S. Penner, M. Armbrüster, Formation of intermetallic compounds by reactive

metal–support interaction: a frequently encountered phenomenon in catalysis, ChemCatChem 7 (2015) 374–392, https://doi.org/10.1002/cctc.201402635.
[212] K. Ploner, L. Schlicker, A. Gili, A. Gurlo, A. Doran, L. Zhang, M. Armbrüster, D. Obendorf, J. Bernardi, B. Klötzer, S. Penner, Reactive metal-support interaction in the Cu-In_2O_3 system: intermetallic compound formation and its consequences for CO_2-selective methanol steam reforming, Sci. Technol. Adv. Mater. 20 (2019) 356–366, https://doi.org/10.1080/14686996.2019.1590127.
[213] K. Föttinger, J.A. van Bokhoven, M. Nachtegaal, G. Rupprechter, Dynamic structure of a working methanol steam reforming catalyst: in situ Quick-EXAFS on Pd/ZnO nanoparticles, J. Phys. Chem. Lett. 2 (2011) 428–433, https://doi.org/10.1021/jz101751s.
[214] A. Haghofer, K. Föttinger, F. Girgsdies, D. Teschner, A. Knop-Gericke, R. Schlögl, G. Rupprechter, In situ study of the formation and stability of supported Pd_2Ga methanol steam reforming catalysts, J. Catal. 286 (2012) 13–21, https://doi.org/10.1016/j.jcat.2011.10.007.
[215] A. Ota, E.L. Kunkes, I. Kasatkin, E. Groppo, D. Ferri, B. Poceiro, R.M. Navarro Yerga, M. Behrens, Comparative study of hydrotalcite-derived supported Pd_2Ga and PdZn intermetallic nanoparticles as methanol synthesis and methanol steam reforming catalysts, J. Catal. 293 (2012) 27–38, https://doi.org/10.1016/j.jcat.2012.05.020.
[216] H. Lorenz, C. Rameshan, T. Bielz, N. Memmel, W. Stadlmayr, L. Mayr, Q. Zhao, S. Soisuwan, B. Klötzer, S. Penner, From oxide-supported palladium to intermetallic palladium phases: consequences for methanol steam reforming, ChemCatChem 5 (2013) 1273–1285, https://doi.org/10.1002/cctc.201200712.
[217] H. Bahruji, M. Bowker, G. Hutchings, N. Dimitratos, P. Wells, E. Gibson, W. Jones, C. Brookes, D. Morgan, G. Lalev, Pd/ZnO catalysts for direct CO_2 hydrogenation to methanol, J. Catal. 343 (2016) 133–146, https://doi.org/10.1016/j.jcat.2016.03.017.
[218] M. Neumann, D. Teschner, A. Knop-Gericke, W. Reschetilowski, M. Armbrüster, Controlled synthesis and catalytic properties of supported In–Pd intermetallic compounds, J. Catal. 340 (2016) 49–59, https://doi.org/10.1016/j.jcat.2016.05.006.
[219] H. Zhou, X. Yang, L. Li, X. Liu, Y. Huang, X. Pan, A. Wang, J. Li, T. Zhang, PdZn intermetallic nanostructure with Pd–Zn–Pd ensembles for highly active and chemoselective semi-hydrogenation of acetylene, ACS Catal. 6 (2016) 1054–1061, https://doi.org/10.1021/acscatal.5b01933.
[220] Y. Cao, Z. Sui, Y. Zhu, X. Zhou, D. Chen, Selective hydrogenation of acetylene over Pd-In/Al_2O_3 catalyst: promotional effect of indium and composition-dependent performance, ACS Catal. 7 (2017) 7835–7846, https://doi.org/10.1021/acscatal.7b01745.
[221] E. Nowicka, S.M. Althahban, Y. Luo, R. Kriegel, G. Shaw, D.J. Morgan, Q. He, M. Watanabe, M. Armbrüster, C.J. Kiely, G.J. Hutchings, Highly selective PdZn/ZnO catalysts for the methanol steam reforming reaction, Catal. Sci. Technol. 8 (2018) 5848–5857, https://doi.org/10.1039/C8CY01100A.
[222] R. Manrique, R. Jiménez, J. Rodríguez-Pereira, V.G. Baldovino-Medrano, A. Karelovic, Insights into the role of Zn and Ga in the hydrogenation of CO_2 to methanol over Pd, Int. J. Hydrogen Energy 44 (2019) 16526–16536, https://doi.org/10.1016/j.ijhydene.2019.04.206.
[223] Z. Li, L. Yu, C. Milligan, T. Ma, L. Zhou, Y. Cui, Z. Qi, N. Libretto, B. Xu, J. Luo, E. Shi, Z. Wu, H. Xin, W.N. Delgass, J.T. Miller, Y. Wu, Two-dimensional transition metal carbides as supports for tuning the chemistry of catalytic nanoparticles, Nat. Commun. 9 (2018) 5258, https://doi.org/10.1038/s41467-018-07502-5.
[224] L. Piccolo, S. Nassreddine, M. Aouine, C. Ulhaq, C. Geantet, Supported Ir–Pd nanoalloys: size–composition correlation and consequences on tetralin hydroconversion properties, J. Catal. 292 (2012) 173–180, https://doi.org/10.1016/j.jcat.2012.05.010.
[225] R.M.J. Fiedorow, B.S. Chahar, S.E. Wanke, The sintering of supported metal catalysts: II. Comparison of sintering rates of supported Pt, Ir, and Rh catalysts in hydrogen and oxygen, J. Catal. 51 (1978) 193–202, https://doi.org/10.1016/0021-9517(78)90293-2.
[226] Y. Nishihata, J. Mizuki, T. Akao, H. Tanaka, M. Uenishi, M. Kimura, T. Okamoto, N. Hamada, Self-regeneration of a Pd-perovskite catalyst for automotive emissions control, Nature 418 (2002) 164–167, https://doi.org/10.1038/nature00893.
[227] C.T. Campbell, S.C. Parker, D.E. Starr, The effect of size-dependent nanoparticle energetics on catalyst sintering, Science 298 (2002) 811–814, https://doi.org/10.1126/science.1075094.
[228] S.R. Challa, A.T. Delariva, T.W. Hansen, S. Helveg, J. Sehested, P.L. Hansen, F. Garzon, A.K. Datye, Relating rates of catalyst sintering to the disappearance of individual nanoparticles during ostwald ripening, J. Am. Chem. Soc. 133 (2011) 20672–20675, https://doi.org/10.1021/ja208324n.
[229] R. Ouyang, J.-X. Liu, W.-X. Li, Atomistic theory of Ostwald ripening and disintegration of supported metal particles under reaction conditions, J. Am. Chem. Soc. 135 (2013) 1760–1771, https://doi.org/10.1021/ja3087054.
[230] S. Nassreddine, L. Massin, M. Aouine, C. Geantet, L. Piccolo, Thiotolerant Ir/SiO_2-Al_2O_3 bifunctional catalysts: effect of metal-acid site balance on tetralin hydroconversion, J. Catal. 278 (2011) 253–265.
[231] L. Piccolo, C. Becker, C.R. Henry, Reaction between CO and a pre-adsorbed oxygen layer on supported palladium clusters, Appl. Surf. Sci. 164 (2000) 156–162, https://doi.org/10.1016/S0169-4332(00)00335-4.
[232] R.M.J. Fiedorow, S.E. Wanke, The sintering of supported metal catalysts: I. Redispersion of supported platinum in oxygen, J. Catal. 43 (1976) 34–42, https://doi.org/10.1016/0021-9517(76)90290-6.
[233] M.A. Newton, Dynamic adsorbate/reaction induced structural change of supported metal nanoparticles: heterogeneous catalysis and beyond, Chem. Soc. Rev. 37 (2008) 2644–2657, https://doi.org/10.1039/B707746G.
[234] A.M. Gänzler, M. Casapu, P. Vernoux, S. Loridant, F.J.C.S. Aires, T. Epicier, B. Betz, R. Hoyer, J.-D. Grunwaldt, Tuning the structure of platinum particles on ceria in situ for enhancing the catalytic performance of exhaust gas catalysts, Angew. Chem. Int. Ed. 56 (2017) 13078–13082, https://doi.org/10.1002/anie.201707842.
[235] Y. Nagai, K. Dohmae, Y. Ikeda, N. Takagi, T. Tanabe, N. Hara, G. Guilera, S. Pascarelli, M.A. Newton, O. Kuno, H. Jiang, H. Shinjoh, S. Matsumoto, In situ redispersion of platinum autoexhaust catalysts: an on-line approach to increasing catalyst lifetimes? Angew. Chem. Int. Ed. 47 (2008) 9303–9306, https://doi.org/10.1002/anie.200803126.
[236] A.M. Gänzler, M. Casapu, F. Maurer, H. Störmer, D. Gerthsen, G. Ferré, P. Vernoux, B. Bornmann, R. Frahm, V. Murzin, M. Nachtegaal, M. Votsmeier, J.-D. Grunwaldt, Tuning the Pt/CeO_2 interface by in situ variation of the Pt particle size, ACS Catal. 8 (2018) 4800–4811, https://doi.org/10.1021/acscatal.8b00330.
[237] H. Tanaka, M. Uenishi, M. Taniguchi, I. Tan, K. Narita, M. Kimura, K. Kaneko, Y. Nishihata, J. Mizuki, The intelligent catalyst having the self-regenerative function of Pd, Rh and Pt for automotive emissions control, Catal. Today 117 (2006) 321–328, https://doi.org/10.1016/j.cattod.2006.05.029.
[238] T.M. Onn, M. Monai, S. Dai, E. Fonda, T. Montini, X. Pan, G.W. Graham, P. Fornasiero, R.J. Gorte, Smart Pd catalyst with improved thermal stability supported on high-surface-area $LaFeO_3$ prepared by atomic layer deposition, J. Am. Chem. Soc. 140 (2018) 4841–4848, https://doi.org/10.1021/jacs.7b12900.
[239] D. Neagu, G. Tsekouras, D.N. Miller, H. Ménard, J.T.S. Irvine, In situ growth of nanoparticles through control of non-stoichiometry, Nat. Chem. 5 (2013) 916–923, https://doi.org/10.1038/nchem.1773.
[240] D. Neagu, T.-S. Oh, D.N. Miller, H. Ménard, S.M. Bukhari, S.R. Gamble, R.J. Gorte, J.M. Vohs, J.T.S. Irvine, Nano-socketed nickel particles with enhanced coking resistance grown in situ by redox exsolution, Nat. Commun. 6 (2015) 8120, https://doi.org/10.1038/ncomms9120.
[241] D. Neagu, V. Kyriakou, I.-L. Roiban, M. Aouine, C. Tang, A. Caravaca, K. Kousi, I. Schreur-Piet, I.S. Metcalfe, P. Vernoux, M.C.M. van de Sanden, M.N. Tsampas, In situ observation of nanoparticle exsolution from perovskite oxides: from atomic scale mechanistic insight to nanostructure tailoring, ACS Nano 13 (2019) 12996–13005, https://doi.org/10.1021/acsnano.9b05652.
[242] L. Liu, D.N. Zakharov, R. Arenal, P. Concepcion, E.A. Stach, A. Corma, Evolution and stabilization of subnanometric metal species in confined space by in situ TEM, Nat. Commun. 9 (2018) 574, https://doi.org/10.1038/s41467-018-03012-6.
[243] K. Morgan, A. Goguet, C. Hardacre, Metal redispersion strategies for recycling of supported metal catalysts: a perspective, ACS Catal. 5 (2015) 3430–3445, https://doi.org/10.1021/acscatal.5b00535.
[244] A. Suzuki, Y. Inada, A. Yamaguchi, T. Chihara, M. Yuasa, M. Nomura, Y. Iwasawa, Time scale and elementary steps of CO-induced disintegration of surface rhodium clusters, Angew. Chem. Int. Ed. 42 (2003) 4795–4799, https://doi.org/10.1002/anie.200352318.
[245] B. Qiao, A. Wang, X. Yang, L.F. Allard, Z. Jiang, Y. Cui, J. Liu, J. Li, T. Zhang, Single-atom catalysis of CO oxidation using Pt_1/FeO_x, Nat. Chem. 3 (2011) 634–641, https://doi.org/10.1038/nchem.1095.
[246] S. Mitchell, E. Vorobyeva, J. Pérez-Ramírez, The multifaceted reactivity of single-atom heterogeneous catalysts, Angew. Chem. Int. Ed. 57 (2018) 15316–15329, https://doi.org/10.1002/anie.201806936.
[247] C. Dessal, L. Martínez, C. Maheu, T. Len, F. Morfin, J.-L. Rousset, E. Puzenat, P. Afanasiev, M. Aouine, L. Soler, J. Llorca, L. Piccolo, Influence of Pt particle size and reaction phase on the photocatalytic performances of ultradispersed Pt/TiO_2 catalysts for hydrogen evolution, J. Catal. 375 (2019) 155–163, https://doi.org/10.1016/j.jcat.2019.05.033.
[248] Z. Jakub, J. Hulva, M. Meier, R. Bliem, F. Kraushofer, M. Setvin, M. Schmid, U. Diebold, C. Franchini, G.S. Parkinson, Local structure and coordination define adsorption in a model Ir_1/Fe_3O_4 single-atom catalyst, Angew. Chem. Int. Ed. 131 (2019) 14099–14106, https://doi.org/10.1002/ange.201907536.
[249] M.K. Samantaray, V. D'Elia, E. Pump, L. Falivene, M. Harb, S. Ould Chikh, L. Cavallo, J.-M. Basset, The comparison between single atom catalysis and surface organometallic catalysis, Chem. Rev. 120 (2019) 734–813, https://doi.org/10.1021/acs.chemrev.9b00238.
[250] G. Kyriakou, M.B. Boucher, A.D. Jewell, E.A. Lewis, T.J. Lawton, A.E. Baber, H.L. Tierney, M. Flytzani-Stephanopoulos, E.C.H. Sykes, Isolated metal atom geometries as a strategy for selective heterogeneous hydrogenations, Science 335 (2012) 1209–1212, https://doi.org/10.1126/science.1215864.
[251] M.T. Greiner, T.E. Jones, S. Beeg, L. Zwiener, M. Scherzer, F. Girgsdies, S. Piccinin, M. Armbrüster, A. Knop-Gericke, R. Schlögl, Free-atom-like d states in single-atom alloy catalysts, Nat. Chem. 10 (2018) 1008–1015, https://doi.org/10.1038/s41557-018-0125-5.
[252] M. Armbrüster, K. Kovnir, M. Friedrich, D. Teschner, G. Wowsnick, M. Hahne, P. Gille, L. Szentmiklósi, M. Feuerbacher, M. Heggen, F. Girgsdies, D. Rosenthal, R. Schlögl, Y. Grin, $Al_{13}Fe_4$ as a low-cost alternative for palladium in heterogeneous hydrogenation, Nat. Mater. 11 (2012) 690–693, https://doi.org/10.1038/nmat3347.
[253] L. Piccolo, L. Kibis, The partial hydrogenation of butadiene over $Al_{13}Fe_4$: a surface-science study of reaction and deactivation mechanisms, J. Catal. 332 (2015) 112–118, https://doi.org/10.1016/j.jcat.2015.09.018.
[254] L. Piccolo, C. Chatelier, M.-C. De Weerd, F. Morfin, J. Ledieu, V. Fournée, P. Gille, E. Gaudry, Catalytic properties of $Al_{13}TM_4$ complex intermetallics: influence of the transition metal and the surface orientation on butadiene hydrogenation, Sci. Technol. Adv. Mater. 20 (2019) 557–567, https://doi.org/10.1080/14686996.2019.1608792.
[255] E. Gaudry, C. Chatelier, D. Loffreda, D. Kandaskalov, A. Coati, L. Piccolo, Catalytic activation of a non-noble intermetallic surface through nanostructuration under hydrogenation conditions revealed by atomistic thermodynamics, J. Mater. Chem.

A (2020), https://doi.org/10.1039/D0TA01146K In press.
[256] G. Jeantelot, M. Qureshi, M. Harb, S. Ould-Chikh, D.H. Anjum, E. Abou-Hamad, A. Aguilar-Tapia, J.-L. Hazemann, K. Takanabe, J.-M. Basset, TiO_2-supported Pt single atoms by surface organometallic chemistry for photocatalytic hydrogen evolution, Phys. Chem. Chem. Phys. 21 (2019) 24429–24440, https://doi.org/10.1039/C9CP04470A.
[257] L. Liu, D.M. Meira, R. Arenal, P. Concepcion, A.V. Puga, A. Corma, Determination of the evolution of heterogeneous single metal atoms and nanoclusters under reaction conditions: which are the working catalytic sites? ACS Catal. 9 (2019) 10626–10639, https://doi.org/10.1021/acscatal.9b04214.
[258] J. Lin, Y. Chen, Y. Zhou, L. Lin, B. Qiao, A. Wang, J. Liu, X. Wang, T. Zhang, More active Ir subnanometer clusters than single-atoms for catalytic oxidation of CO at low temperature, AIChE J. 63 (2017) 4003–4012, https://doi.org/10.1002/aic.15756.
[259] S. Duan, R. Wang, J. Liu, Stability investigation of a high number density Pt_1/Fe_2O_3 single-atom catalyst under different gas environments by HAADF-STEM, Nanotechnology 29 (2018) 204002, , https://doi.org/10.1088/1361-6528/aab1d2.
[260] A. Liu, L. Liu, Y. Cao, J. Wang, R. Si, F. Gao, L. Dong, Controlling dynamic structural transformation of atomically dispersed CuO_x species and influence on their catalytic performances, ACS Catal. 9 (2019) 9840–9851, https://doi.org/10.1021/acscatal.9b02773.
[261] K. Ding, A. Gulec, A.M. Johnson, N.M. Schweitzer, G.D. Stucky, L.D. Marks, P.C. Stair, Identification of active sites in CO oxidation and water-gas shift over supported Pt catalysts, Science 350 (2015) 189–192, https://doi.org/10.1126/science.aac6368.
[262] Y. Guo, S. Mei, K. Yuan, D.-J. Wang, H.-C. Liu, C.-H. Yan, Y.-W. Zhang, Low-temperature CO_2 methanation over CeO_2-supported Ru single atoms, nanoclusters, and nanoparticles competitively tuned by strong metal–support interactions and H-spillover effect, ACS Catal. 8 (2018) 6203–6215, https://doi.org/10.1021/acscatal.7b04469.
[263] E.D. Goodman, A.C. Johnston-Peck, E.M. Dietze, C.J. Wrasman, A.S. Hoffman, F. Abild-Pedersen, S.R. Bare, P.N. Plessow, M. Cargnello, Catalyst deactivation via decomposition into single atoms and the role of metal loading, Nat. Catal. 2 (2019) 748–755, https://doi.org/10.1038/s41929-019-0328-1.
[264] H. Wang, J.-X. Liu, L.F. Allard, S. Lee, J. Liu, H. Li, J. Wang, J. Wang, S.H. Oh, W. Li, M. Flytzani-Stephanopoulos, M. Shen, B.R. Goldsmith, M. Yang, Surpassing the single-atom catalytic activity limit through paired Pt-O-Pt ensemble built from isolated Pt_1 atoms, Nat. Commun. 10 (2019) 1–12, https://doi.org/10.1038/s41467-019-11856-9.
[265] L. DeRita, J. Resasco, S. Dai, A. Boubnov, H.V. Thang, A.S. Hoffman, I. Ro, G.W. Graham, S.R. Bare, G. Pacchioni, X. Pan, P. Christopher, Structural evolution of atomically dispersed Pt catalysts dictates reactivity, Nat. Mater. 18 (2019) 746, https://doi.org/10.1038/s41563-019-0349-9.
[266] J. Gu, C.-S. Hsu, L. Bai, H.M. Chen, X. Hu, Atomically dispersed Fe^{3+} sites catalyze efficient CO_2 electroreduction to CO, Science 364 (2019) 1091–1094, https://doi.org/10.1126/science.aaw7515.
[267] A.S. Varela, W. Ju, A. Bagger, P. Franco, J. Rossmeisl, P. Strasser, Electrochemical reduction of CO_2 on metal-nitrogen-doped carbon catalysts, ACS Catal. 9 (2019) 7270–7284, https://doi.org/10.1021/acscatal.9b01405.
[268] L. Huang, J. Chen, L. Gan, J. Wang, S. Dong, Single-atom nanozymes, Sci. Adv. 5 (2019) eaav5490, , https://doi.org/10.1126/sciadv.aav5490.
[269] D. Karapinar, N.T. Huan, N.R. Sahraie, J. Li, D. Wakerley, N. Touati, S. Zanna, D. Taverna, L.H.G. Tizei, A. Zitolo, F. Jaouen, V. Mougel, M. Fontecave, Electroreduction of CO_2 on single-site copper-nitrogen-doped carbon material: selective formation of ethanol and reversible restructuration of the metal sites, Angew. Chem. Int. Ed. 58 (2019) 15098–15103, https://doi.org/10.1002/anie.201907994.
[270] Z. Chen, E. Vorobyeva, S. Mitchell, E. Fako, M.A. Ortuño, N. López, S.M. Collins, P.A. Midgley, S. Richard, G. Vilé, J. Pérez-Ramírez, A heterogeneous single-atom palladium catalyst surpassing homogeneous systems for Suzuki coupling, Nat. Nanotechnol. 13 (2018) 702, https://doi.org/10.1038/s41565-018-0167-2.
[271] B. Zandkarimi, A.N. Alexandrova, Dynamics of subnanometer Pt clusters can break the scaling relationships in catalysis, J. Phys. Chem. Lett. 10 (2019) 460–467, https://doi.org/10.1021/acs.jpclett.8b03680.
[272] A. Khorshidi, J. Violet, J. Hashemi, A.A. Peterson, How strain can break the scaling relations of catalysis, Nat. Catal. 1 (2018) 263–268, https://doi.org/10.1038/s41929-018-0054-0.